

1. Report No. FHWA/TX-13/5-5123-03-1		2. Government Accession No.		3. Recipient's Catalog No.	
4. Title and Subtitle IMPLEMENTATION OF TEXAS ASPHALT CONCRETE OVERLAY DESIGN SYSTEM				5. Report Date Published: August 2014	
				6. Performing Organization Code	
7. Author(s) Sheng Hu, Fujie Zhou, and Tom Scullion				8. Performing Organization Report No. Report 5-5123-03-1	
9. Performing Organization Name and Address Texas A&M Transportation Institute College Station, Texas 77843-3135				10. Work Unit No. (TRAIS)	
				11. Contract or Grant No. Project 5-5123-03	
12. Sponsoring Agency Name and Address Texas Department of Transportation Research and Technology Implementation Office P. O. Box 5080 Austin, Texas 78763-5080				13. Type of Report and Period Covered Technical Report: Mar. 2009–Aug. 2012	
				14. Sponsoring Agency Code	
15. Supplementary Notes Project performed in cooperation with the Texas Department of Transportation and the Federal Highway Administration. Project Title: Pilot Implementation of the New Asphalt Overlay Design System URL: http://tti.tamu.edu/documents/5-5123-03-1.pdf					
16. Abstract An asphalt overlay design system was developed for Texas Department of Transportation (TxDOT) under Research Project 0-5123. The new overlay design system, named the Texas Asphalt Concrete Overlay Design System (TxACOL), can help pavement engineers optimize asphalt overlay design in terms of overlay mix type and thickness, based upon existing pavement structure and conditions (existing distress types and/or load transfer efficiency at joints/cracks), local weather conditions, and anticipated traffic level. Several districts in Texas expressed interest in implementing this new overlay design system for designing asphalt overlays. To facilitate the implementation in districts, Project 5-5123-03 was initiated. The work performed under this study included (a) developing and conducting district-oriented overlay design workshops, (b) providing asphalt overlay design assistance and monitoring the new constructed overlays, (c) performing laboratory testing and updating the material default values of overlay mixes, (d) surveying the field performance (rutting and cracking) of asphalt overlay projects, and (e) enhancing and calibrating the TxACOL. This report documents the work and findings from this study. Case analyses showed that the enhanced TxACOL can make reasonable predictions compared to survey results. The researchers recommend that TxACOL be used as a tool for asphalt overlay design in TxDOT districts. Apparently, calibration factors still need to be further verified through more field test sections.					
17. Key Words TxACOL, Overlay Design, Asphalt, Rutting, Cracking, Implementation				18. Distribution Statement No restrictions. This document is available to the public through NTIS: National Technical Information Service Alexandria, Virginia 22312 http://www.ntis.gov	
19. Security Classif. (of this report) Unclassified	20. Security Classif. (of this page) Unclassified		21. No. of Pages 102	22. Price	

IMPLEMENTATION OF TEXAS ASPHALT CONCRETE OVERLAY DESIGN SYSTEM

by

Sheng Hu, Ph.D., P.E.
Assistant Research Engineer
Texas A&M Transportation Institute

Fujie Zhou, Ph.D., P.E.
Associate Research Engineer
Texas A&M Transportation Institute

and

Tom Scullion, P.E.
Senior Research Engineer
Texas A&M Transportation Institute

Report 5-5123-03-1
Project 5-5123-03
Project Title: Pilot Implementation of the New Asphalt Overlay Design System

Performed in cooperation with the
Texas Department of Transportation
and the
Federal Highway Administration

Published: August 2014

TEXAS A&M TRANSPORTATION INSTITUTE
College Station, Texas 77843-3135

DISCLAIMER

The contents of this report reflect the views of the authors, who are responsible for the facts and the accuracy of the data presented here. The contents do not necessarily reflect the official view or policies of the Federal Highway Administration (FHWA) or the Texas Department of Transportation (TxDOT). This report does not constitute a standard, specification, or regulation, nor is it intended for construction, bidding, or permit purposes.

The United States Government and the State of Texas do not endorse products or manufacturers. Trade or manufacturers' names appear herein solely because they are considered essential to the object of this report.

The researcher in charge was Sheng Hu, P.E. (Texas, #103577).

ACKNOWLEDGMENTS

This project was made possible by the Texas Department of Transportation in cooperation with the Federal Highway Administration. In particular, the guidance and technical assistance provided by the project director (PD), Dar-Hao Chen, Ph.D., P.E., of TxDOT proved invaluable. The following project advisors also provided valuable input throughout the course of the project, and their technical assistance is acknowledged:

- German Claros, Ph.D, P.E., Research Technology and Implementation Office.
- Joe Leidy, P.E., Construction Division.
- Magdy Mikhail, Ph.D, P.E., Maintenance Division.
- Feng Hong, Ph.D, P.E., Construction Division.

TABLE OF CONTENTS

	Page
List of Figures	ix
List of Tables	xii
List of Abbreviations	xiii
Chapter 1. Introduction	1
1.1 Background and Objectives	1
1.2 Report Organization.....	2
Chapter 2. Overview of Completed Work	3
2.1 Workshops	3
2.2 Field Performance Survey.....	4
2.3 Overlay Design Assistance	6
2.4 Program Enhancement.....	6
2.5 Summary	7
Chapter 3. Field Survey Data Analysis	9
3.1 Introduction.....	9
3.2 Crack Survey Data Format.....	9
3.3 Definition of RCR (%).....	11
3.4 Survey Results of Pumphrey Street	12
3.5 Survey Results of SH 12	20
3.6 Survey Results of US 82	24
3.7 Survey Results of SH 24	26
3.8 Survey Results of IH 40.....	28
3.9 Survey Results of SH 359	31
3.10 Survey Results of US 87	33
3.11 Summary	37
Chapter 4. Determination of Key Input Parameters.....	39
4.1 Dynamic Modulus.....	39
4.2 Fracture Property	42
4.3 Rutting Property.....	46
4.4 FWD Modulus	48

4.5 LTE	50
4.6 Default Values	53
4.7 Summary	55
Chapter 5. TXACOL Enhancement	57
5.1 Workshop Feedback.....	57
5.2 New RCR Model.....	57
5.3 New Thermal SIF Model Accounting for the Influence of Thick CTB Layer	60
5.4 LTE Standard Deviation Consideration.....	63
5.5 Calibration Factors.....	64
5.6 Summary	68
Chapter 6. Case Studies	69
6.1 Case 1: IH 40 Test Sections	69
6.2 Case 2: SH 24 Test Section.....	77
6.3 Summary	84
Chapter 7. Conclusions and Recommendations.....	85
References	87

LIST OF FIGURES

Figure	Page
Figure 2-1. Cover of Product 5-5123-03-P1.	4
Figure 2-2. Districts Involved during 5-5123-03 Project Period.	8
Figure 3-1. Cracking Data Format.	10
Figure 3-2. RCR Concept.	12
Figure 3-3. Schematic Diagram of Pumphrey Street Pavement Structure.....	12
Figure 3-4. Plan View of Pumphrey Street Sections (drawing not to scale).	14
Figure 3-5. Photo of Pumphrey Street Sections (taken from overpass, facing north).	15
Figure 3-6. Photo of Pumphrey Street Sections (taken from overpass, facing south).	15
Figure 3-7. Photos of the Same Crack in Pumphrey Street on Each Survey Date.	17
Figure 3-8. RCR vs. Months of Pumphrey Street Main Road Sections.	19
Figure 3-9. RCR vs. Months of Pumphrey Street Ramp Sections.....	20
Figure 3-10. Schematic Diagram of SH 12 Pavement Structure.	20
Figure 3-11. SH 12 Test Section Overview.	21
Figure 3-12. Photos of the Same Crack in SH 12 on Each Survey Date	22
Figure 3-13. Rut Measurement on SH 12.	23
Figure 3-14. SH 12 RCR (%) vs. Months.	24
Figure 3-15. Schematic Diagram of US 82 Pavement Structure.	24
Figure 3-16. US 82 Overlay Section Overview.	25
Figure 3-17. US 82 Rut Measurement.	25
Figure 3-18. Schematic Diagram of SH 24 Pavement Structure.	26
Figure 3-19. Overview of SH 24 Test Section.....	26
Figure 3-20. Photos of the Same Crack in SH 24 on Each Survey Date.	27
Figure 3-21. SH 24 RCR (%) vs. Months.	28
Figure 3-22. Schematic Diagram of IH 40 Pavement Structure.	28
Figure 3-23. Overview of IH 40 Test Sections.	29
Figure 3-24. Photos of the Same Crack on IH 40 on Each Survey Date.	30
Figure 3-25. RCR vs. Months on IH 40 Test Sections.	31
Figure 3-26. Schematic Diagram of SH 359 Pavement Structure.	32

Figure 3-27. Overview of SH 359 Test Section.....	32
Figure 3-28. No Crack, No Rutting in SH 359 Test Section, as of 5/24/2012.	33
Figure 3-29. Schematic Diagram of US 87 Pavement Structure.	33
Figure 3-30. Overview of US 87 Test Sections.	34
Figure 3-31. Photos of the Same Crack in US 87 on Each Survey Date.	35
Figure 3-32. No Rutting in US 87 Test Sections, as of 5/30/2012.	36
Figure 3-33. RCR vs. Months for US 87 Test Sections.....	37
Figure 4-1. Dynamic Modulus Test Equipment and Specimen.....	40
Figure 4-2. Dynamic Modulus Input Interface.	41
Figure 4-3. Dynamic Modulus Master Curve and Equations.	42
Figure 4-4. A and n Determination.	43
Figure 4-5. A and n Input Interface.	44
Figure 4-6. Interface of A and n Analysis Tool with Multiple OT Data File Handling.	45
Figure 4-7. Output of the OT A and n Analysis Tool.....	45
Figure 4-8. Permanent Micro Strain vs. Number of Load Repetition.	46
Figure 4-9. Rutting Property Input Interface.	47
Figure 4-10. Excel Macro for Determining Rutting Properties.	48
Figure 4-11. An Example of Regular Deflection Basin.....	49
Figure 4-12. An Example of Irregular Deflection Basin.	49
Figure 4-13. An Example of Back-Calculation Result.	50
Figure 4-14. FWD Back-Calculated Modulus Input Interface.	50
Figure 4-15. FWD Test with the Loading Plate at One Side of Crack.	51
Figure 4-16. Schematic Diagram of W1c, W2c, W1j, and W2j.	51
Figure 4-17. LTE Determination Based on FWD Data.	52
Figure 4-18. LTE Input Interface.....	53
Figure 5-1. RCR Curves Determined by Previous TxACOL, after (<i>I</i>).	58
Figure 5-2. Curves of RCR Model ($\rho = 120$).....	60
Figure 5-3. Cracked CTB Layer.	61
Figure 5-4. Three-Layer AC/Existing AC/CTB Pavement Structure Thermal SIF Model.	61
Figure 5-5. CTE Input for CTB Layer.	63
Figure 5-6. RCR Curves Accounting for LTE STD.	64

Figures 5-7. Influence of Overlay Mix Type.	65
Figures 5-8. Influence of Overlay Thickness.	66
Figure 5-9. Influence of Traffic.	66
Figure 5-10. Influence of LTE STD.	67
Figure 6-1. Existing Pavement Condition of IH 40 Test Sections.	69
Figure 6-2. Crack Survey Recording Excel File for IH 40 Test Section.	70
Figure 6-3. FWD Test on IH 40 Test Sections.	71
Figure 6-4. Input Parameters for Modulus Back-Calculation.	72
Figure 6-5. Station Selection for Modulus Back-Calculation.	72
Figure 6-6. Modulus Back-Calculation Result.	73
Figure 6-7. RCR Prediction and Survey Result of IH 40 Test Section 1.	76
Figure 6-8. RCR Prediction and Survey Result of IH 40 Test Section 2.	76
Figure 6-9. RCR Prediction and Survey Result of IH 40 Test Section 3.	77
Figure 6-10. Cracking Map of SH 24 Test Section before Asphalt Overlay Construction.	78
Figure 6-11. SH 24 Overlay Asphalt Mix Design Sheet.	79
Figure 6-12. HWTT Results.	80
Figure 6-13. CTE Measuring of CTB Material.	82
Figure 6-14. RCR Prediction and Survey Result of SH 24 Test Section.	83
Figure 6-15. SH 24 Rut Prediction Result.	83

LIST OF TABLES

Table	Page
Table 3-1. Crack Number of Pumphrey Street Main Road Sections.....	18
Table 3-2. Crack Number of Pumphrey Street Ramp Sections.	18
Table 3-3. RCR (%) of Pumphrey Street Main Road Sections.....	18
Table 3-4. RCR (%) of Pumphrey Street Ramp Sections.....	19
Table 3-5. Crack Number and RCR (%) of SH 12 during Each Survey.	23
Table 3-6. Rut Depth (mm) of US 82 at Wheel Path during Each Survey.....	26
Table 3-7. Crack Number and RCR (%) of SH 24 during Each Survey.	27
Table 3-8. RCR (%) of IH 40 Test Sections during Each Survey.	31
Table 3-9. RCR of US 87 Test Sections during Each Survey.	36
Table 4-1. Sample $ E^* $ Values (ksi).....	40
Table 4-2. Default Values.	54
Table 6-1. LTE Values for IH 40 Test Sections.	73
Table 6-2. Dynamic Modulus (ksi) for IH 40 Test Section 1 (0% RAP, PG 64-28).....	74
Table 6-3. Dynamic Modulus (ksi) for IH 40 Test Section 2 (35% RAP, AC-10).	74
Table 6-4. Dynamic Modulus (ksi) for IH 40 Test Section 3 (20% RAP, PG 64-28).....	74
Table 6-5. A and n Values for IH 40 Test Sections.....	75
Table 6-6. Cracking Properties.	81
Table 6-7. Dynamic Modulus Results (ksi).....	81
Table 6-8. Rutting Properties.....	81

LIST OF ABBREVIATIONS

AC	Asphalt Concrete
CAM	Crack Attenuation Mix
CMHB	Coarse Matrix High Binder
CTB	Cement-Treated Base
CTE	Coefficient of Thermal Expansion
ESAL	Equivalent Single Axle Load
FHWA	Federal Highway Administration
FWD	Falling Weight Deflectometer
GPS	Global Positioning System
HMA	Hot-Mix Asphalt
HWTT	Hamburg Wheel Tracking Test
JPCP	Jointed Plain Concrete Pavement
LTE	Load Transfer Efficiency
LTE STD	Load Transfer Efficiency Standard Deviation
LVDT	Linear Variable Differential Transformer
NCHRP	National Cooperative Highway Research Program
OT	Overlay Test
PCC	Portland Cement Concrete
PFC	Porous Friction Concrete

RAP	Reclaimed Asphalt Pavement
RAS	Recycled Asphalt Shingle
RCR	Reflective Cracking Rate
SBR	Styrene-Butadiene Rubber
SIF	Stress Intensity Factor
SMA	Stone Mastic Asphalt
SMAR	Stone-Matrix Asphalt Rubber
TTI	Texas A&M Transportation Institute
TxACOL	Texas Asphalt Concrete Overlay Design System
TxDOT	Texas Department of Transportation

CHAPTER 1.

INTRODUCTION

1.1 BACKGROUND AND OBJECTIVES

The placement of an asphalt overlay is the most common method used by the Texas Department of Transportation (TxDOT) to rehabilitate existing asphalt and concrete pavements. Determining the type of overlay mix and its required thickness are important decisions that TxDOT engineers make on a daily basis. However, the decision process sometimes is a difficult task because for an asphalt overlay to perform well, it must have a balance of good rut and crack resistance.

Furthermore, the overlay performance is highly influenced by many factors, such as existing pavement conditions, traffic loading, and environmental conditions. To assist TxDOT engineers in making rational decisions, researchers developed the Texas Asphalt Concrete Overlay Design System (TxACOL) under Research Project 0-5123, “Development of an Advanced Asphalt Overlay Design System Incorporating Both Reflection Cracking and Rutting Requirements.”

Two major distresses of asphalt overlays—reflective cracking and rutting—are predicted simultaneously by the TxACOL program, with full consideration of the influential factors.

Several TxDOT districts expressed interest in implementing the TxACOL for designing asphalt overlays. To facilitate the implementation of the TxACOL overlay design, TxDOT initiated this implementation project, 5-5123-03, “Pilot Implementation of the New Asphalt Overlay Design System.” The objectives of this implementation project were to:

- Develop and conduct district-oriented overlay design workshops for user training and user feedback.
- Provide asphalt overlay design assistance in terms of lab testing/existing pavement evaluation and monitoring of the construction of the new overlay test sections.
- Evaluate district-provided materials and updating of the material default value database.
- Survey/monitor the field performance (rutting and cracking) of existing asphalt overlay projects.
- Upgrade/calibrate the new asphalt overlay design system.

1.2 REPORT ORGANIZATION

This report is organized into the following seven chapters.

- Chapter 1: Introduction—provides a brief description of the project background, objectives, and report organization.
- Chapter 2: Overview of Completed Tasks—summarizes the overall work and accomplishments during the period of the research project, which include workshops, field surveys, lab tests, and system updates/calibrations, etc.
- Chapter 3: Field Survey Data Analysis—presents detailed information about field survey data (cracking/rutting) of existing overlay test sections and associated analysis.
- Chapter 4: Determination of Key Input Parameters—discusses the determination methods/tools for some key input parameters such as dynamic modulus, cracking/rutting properties, and load transfer efficiency (LTE) at cracks/joints, etc. Based on significant lab testing on different overlay mixes sent from districts, default values of some key inputs are presented in this chapter.
- Chapter 5: TxACOL Enhancement—describes the system upgrading and calibration. Workshop feedback, default values, and field survey data analysis findings were all addressed or incorporated in the updated software, and some new models were proposed and integrated into the updated program as well.
- Chapter 6: Case Studies—compares the prediction from the enhanced, updated system with the field-observed performance of several overlay test sections.
- Chapter 7: Conclusions and Recommendations—presents conclusions and recommendations based on the findings of this research project.

CHAPTER 2.

OVERVIEW OF COMPLETED WORK

This chapter gives an overview of the completed work, which includes:

- Training workshop development for districts.
- Field performance monitoring for all the available overlay test sections.
- Overlay design assistance to districts.
- TxACOL program enhancement.

Findings and achievements from each working task are briefly described in this chapter as well.

2.1 WORKSHOPS

Five workshops were conducted for five different districts:

- Paris District, August 25, 2009.
- Austin District, October 6, 2009.
- Lubbock District, September 9, 2010.
- Beaumont District, June 2, 2011.
- Odessa District, February 16, 2012.

For each workshop, TxDOT engineers (pavement design engineers, pavement management engineers, and/or lab engineers) from the host district and adjacent districts attended the workshop. The workshop training materials were developed to help users in three aspects: (1) understanding the basic principle of the TxACOL overlay design system, (2) knowing how to use the TxACOL program to design an overlay, and (3) getting in-depth knowledge about both necessary lab and field testing to obtain key input parameters.

Specifically, the district-oriented case examples and exercises were carefully designed for each workshop. These sample cases were targeted to incorporate local weather station data, common pavement structure, and typical materials, as specific as possible for the host district. The trainees also had chances to practice the exercises on their own during the workshop.

Researchers collected and then addressed user feedback when updating the TxACOL program.

The workshop training materials were submitted as Product 5-5123-03-P1 and were then published in August 2011. See Figure 2-1.

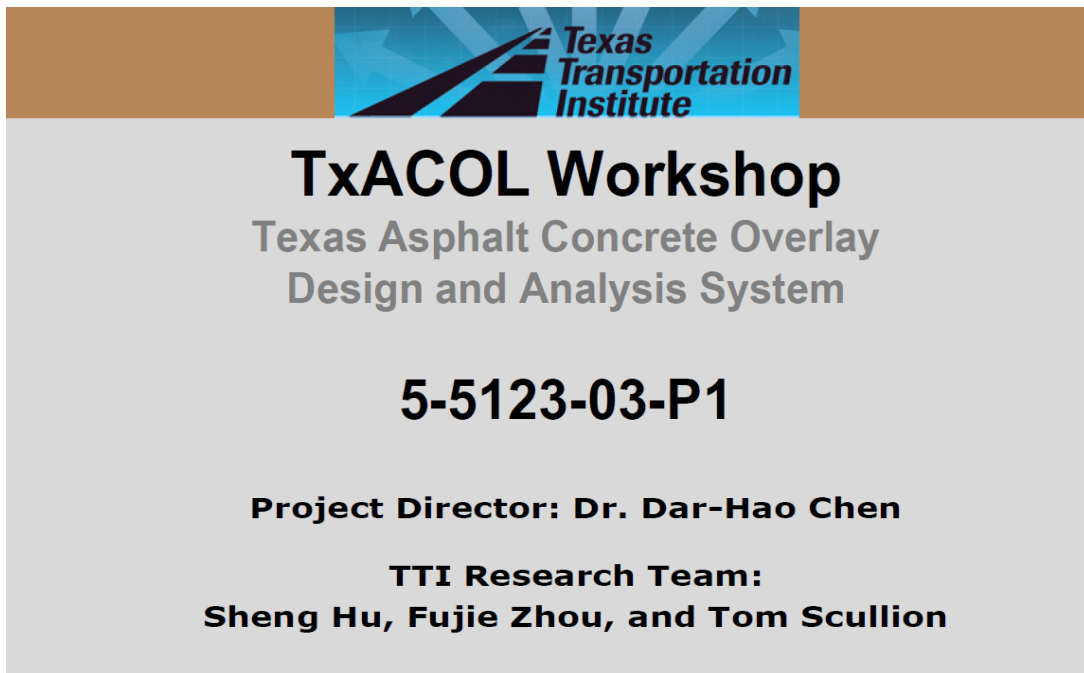


Figure 2-1. Cover of Product 5-5123-03-P1.

2.2 FIELD PERFORMANCE SURVEY

One of the main tasks of Project 5-5123-03 was to monitor the field performances of overlay test sections in terms of rutting and cracking. The observed field performance data are crucial to update and recalibrate the TxACOL prediction models. Researchers identified 18 overlay test sections for continuous performance monitoring, including 10 existing test sections (constructed before the research project start date) and eight new test sections (constructed after the research project start date).

The 10 existing test sections and associated survey dates are:

- Beaumont District: SH 12, one test section.
 - Six surveys were conducted, in December 2009, April 2010, November 2010, June 2011, October 2011, and May 2012.
- Wichita Falls District: US 82, one test section.

- Six surveys were conducted, in December 2009, April 2010, November 2010, April 2011, December 2011, and July 2012.
- Fort Worth District: Pumphrey Street, eight test sections.
 - Six surveys were conducted, in December 2009, May 2010, September 2010, April 2011, December 2011, and July 2012.

The eight new test sections and associated survey dates are:

- Paris District: SH 24, one test section.
 - Four surveys were conducted, in April 2010, December 2010, June 2011, and December 2011.
- Laredo District: SH 359, one test section.
 - Four surveys were conducted, in November 2010, April 2011, December 2011, and May 2012.
- Amarillo District: IH 40, four test sections.
 - Five surveys were conducted, in April 2010, September 2010, April 2011, December 2011, and May 2012.
- Amarillo District: US 87, two test sections.
 - Three surveys were conducted, in April 2011, December 2011, and May 2012.

The field surveys included visual observation and photos, as well as rutting and cracking measurements. For each test section, the surveys were conducted twice a year; one right after summer when the rut depth could potentially develop, and the other after winter when the crack number could grow.

In each test section, the start and ending points were carefully marked based on global positioning system (GPS) coordinates or some permanent reference points. Then the rolling distance measuring wheel was employed to measure the distance from start point to locate every crack, and each observed crack was photographed during each survey. All the survey data were organized in Excel format.

Chapter 3 presents more detailed survey information and analyses for each test section.

2.3 OVERLAY DESIGN ASSISTANCE

The assistance provided for districts regarding overlay design covered four aspects: (1) overlay mixture design, (2) existing pavement condition evaluation, (3) overlay construction monitoring, and (4) plant mix characterization.

During the period of Project 5-5123-03, the researchers assisted six districts with overlay mix design and characterization. In the last several years, Texas districts have used many reclaimed asphalt pavement/recycled asphalt shingle (RAP/RAS) mixes for asphalt overlays. The mixes evaluated under this study included:

- Three RAP/RAS mixes from the Paris District.
- One RAP mix from the Laredo District.
- Four virgin mixes from the Odessa District.
- Four RAP mixes from the Lubbock District.
- Two virgin mixes from the Dallas District.
- Three RAP mixes from the Amarillo District.

For each mix evaluation, a dynamic modulus test, overlay test, Hamburg test, and repeated load test were performed to characterize the mixture modulus, cracking properties, and rutting properties. Based on these data, the researchers updated/proposed default values for some mixtures.

Several technical memorandums documented the lab test results, such as *SH 24 Asphalt Overlay Investigation and Model Prediction*, submitted on May 19, 2010, and *Sampling, Lab Testing, and Evaluation for SH 11 Asphalt Overlay Mixture*, submitted on July 5, 2011. More detailed information about the lab testing and existing pavement condition evaluation is provided in Chapter 4, from the TxACOL implementation point of view.

2.4 PROGRAM ENHANCEMENT

The TxACOL program enhancements included the following items.

- User-interface improvement. Based on the trainees' feedback during the workshops, the researchers made corresponding modifications to make the program more user friendly. Some bugs and problematic logic issues were also fixed and optimized.

- New model development. Two new models were developed and proposed during this research project period. One is a new thermal stress intensity factor (SIF) model to account for the influence of a very thick cement-treated base (CTB) layer, which was not considered in the previous TxACOL system; the other is a new reflective cracking rate (RCR) model that fits better to the observed field performance data than the previous model. The RCR calculation algorithm was also improved to account for the influence of standard deviation of LTE at cracks/joints.
- Updated default values. Through the assistance for district overlay design, the researchers gathered more lab testing data for different asphalt mixtures and updated the default values of some inputs. The new default values were incorporated into the program to help engineers make better estimations of asphalt mixes during overlay design.
- Calibration factor refinement. Based on numerous pilot calculations and sensitivity analyses, the calibration factors were refined.

Chapter 5 discusses detailed information about program enhancement.

2.5 SUMMARY

This chapter summarized the working tasks completed in this research project. To assist districts in implementing TxACOL for overlay design, the researchers conducted four tasks: (1) district-oriented workshops, (2) field performance surveys, (3) overlay design assistance including overlay mixture design/characterization and existing pavement condition evaluation, and (4) program enhancement. The purpose of all these working tasks was to help districts design optimum overlays for project-specific service conditions.

Figure 2-2 pinpoints the involved districts during this project. The researchers appreciated the cooperation of these districts, as well as the coordinated efforts of the project director, panel members, and district pavement and/or materials engineers. The involvement of more districts will undoubtedly assure better implementation results.

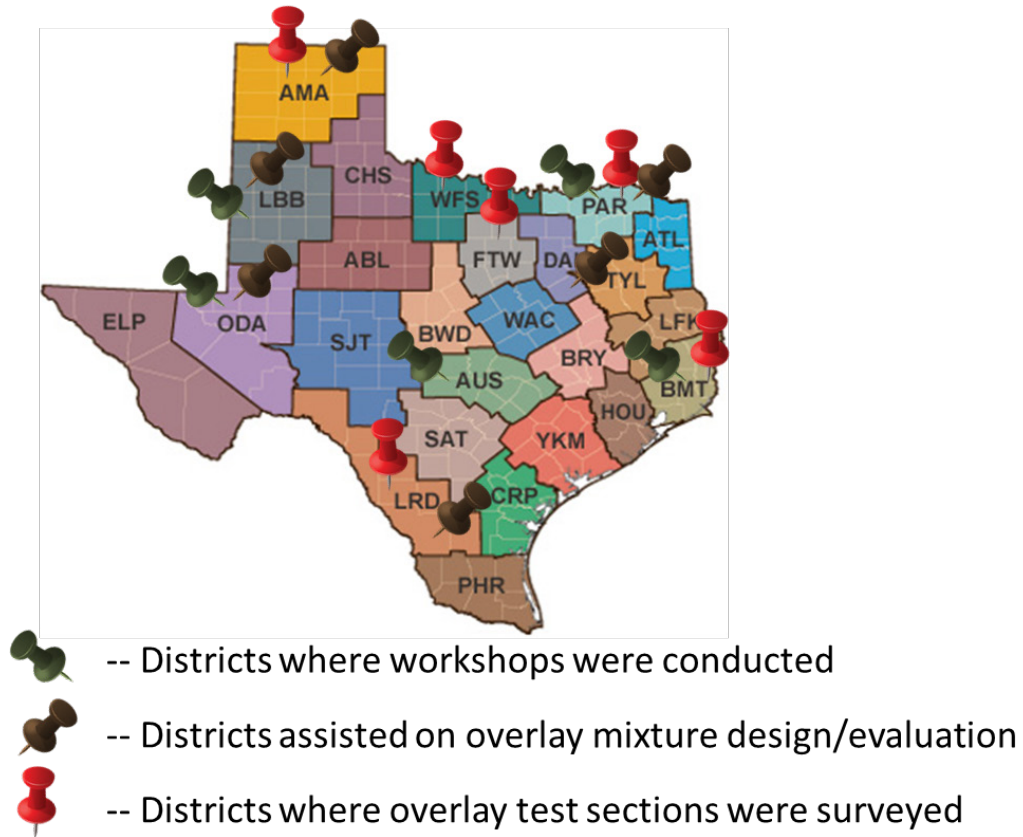


Figure 2-2. Districts Involved during 5-5123-03 Project Period.

CHAPTER 3.

FIELD SURVEY DATA ANALYSIS

3.1 INTRODUCTION

Visual survey, cracking, and rutting measurements were conducted twice a year for identified overlay test sections. From 2009 to 2012, 10 existing overlay sections, including Pumphrey Street (eight test sections) in the Fort Worth District, SH 12 (one test section) in the Beaumont District, and US 82 (one test section) in the Wichita Falls District, were monitored. From 2010 to 2012, eight new overlay sections, including SH 24 (one test section) in the Paris District, IH 40 (four test sections) and US 87 (two test sections) in the Amarillo District, and SH 359 (one test section) in the Laredo District, were also identified and continuously monitored.

For the asphalt overlay test sections on Pumphrey Street, SH 12, SH 24, IH 40, and US 87, reflective cracking was the dominant distress. However, the asphalt overlay on US 82 performed excellent after nine years of service under very heavy traffic; it had no crack at all except that some rutting was observed on the uphill area. For the RAP test section on SH 359, the overlay still performed very well in the last survey, and no crack or rutting was observed.

Since cracking was the dominant distress observed in these test sections, this chapter focuses on the crack development of each test section and associated analysis. In this chapter, the crack survey data format is illustrated first, then the definition of reflective cracking rate is explained, and then the survey result for each test section is presented.

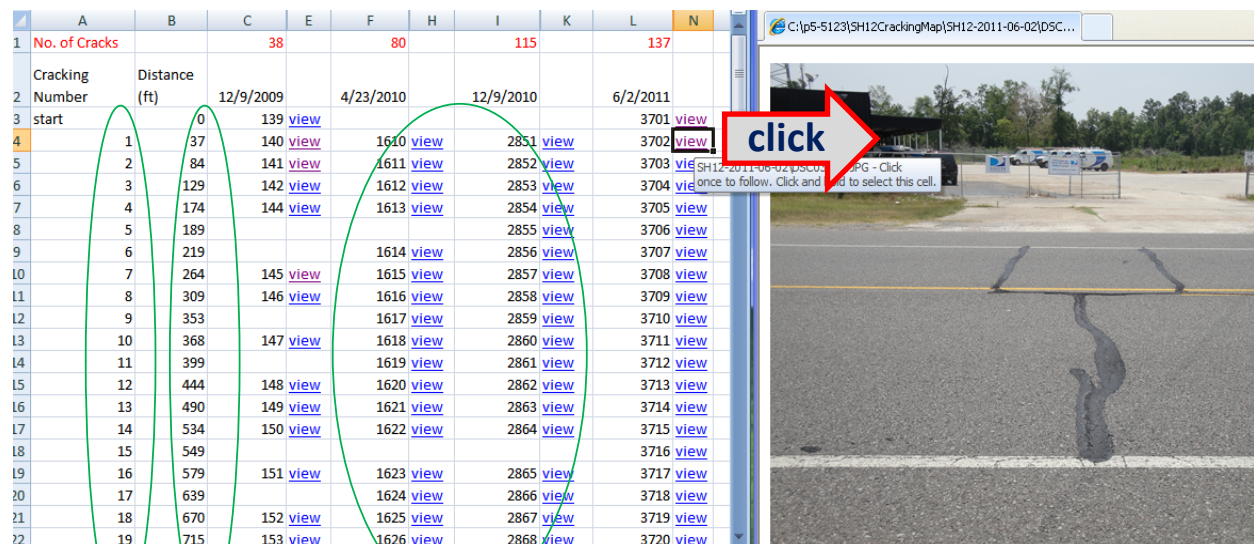
3.2 CRACK SURVEY DATA FORMAT

For each test section, researchers carefully marked the start and end point based on GPS coordinates or some permanent reference signs. For cracked test sections, the rolling distance measuring wheel was employed to measure the distance from start point to locate every crack. Each crack was photographed during each survey. All the survey data were organized in Excel format and included the crack number, distance from start point, and crack photo number. In the Excel file, the corresponding photo pops up when the photo number is clicked (see Figure 3-1).

In Figure 3-1, the first line shows the total crack number for each survey. For example, the total numbers of observed cracks are 38 on December 9, 2009, 80 on April 23, 2010, and 115 on December 9, 2010, and June 2, 2011.

For each crack, the distance from the start point to that specific crack is listed in the second column. For example, crack 1 is 37 ft away from the start point. The photo numbers for crack 1 are 140, 1610, 2851, and 3702, corresponding to each survey, respectively. If users click the “view” link close to the cell that reads “3702” (photo number), the photo of crack 1 taken on June 2, 2012, will pop up.

In this way, researchers were able to document and organize each crack history. For example, researchers could easily identify that crack 5 (189 ft away from the start point) was a new crack after April 23, 2010, and was observed on and after December 9, 2010.



	A	B	C	E	F	H	I	K	L	N
1	No. of Cracks		38		80		115		137	
2	Cracking Number	Distance (ft)	12/9/2009		4/23/2010		12/9/2010		6/2/2011	
3	start	0	139	view					3701	view
4	1	37	140	view	1610	view	2851	view	3702	view
5	2	84	141	view	1611	view	2852	view	3703	view
6	3	129	142	view	1612	view	2853	view	3704	view
7	4	174	144	view	1613	view	2854	view	3705	view
8	5	189					2855	view	3706	view
9	6	219			1614	view	2856	view	3707	view
10	7	264	145	view	1615	view	2857	view	3708	view
11	8	309	146	view	1616	view	2858	view	3709	view
12	9	353			1617	view	2859	view	3710	view
13	10	368	147	view	1618	view	2860	view	3711	view
14	11	399			1619	view	2861	view	3712	view
15	12	444	148	view	1620	view	2862	view	3713	view
16	13	490	149	view	1621	view	2863	view	3714	view
17	14	534	150	view	1622	view	2864	view	3715	view
18	15	549							3716	view
19	16	579	151	view	1623	view	2865	view	3717	view
20	17	639			1624	view	2866	view	3718	view
21	18	670	152	view	1625	view	2867	view	3719	view
22	19	715	153	view	1626	view	2868	view	3720	view

Crack No. Distance Photo No.

Figure 3-1. Cracking Data Format.

Since tens of thousands of photos were stored and organized during the surveys, the total survey data volume was more than 16 GB.

3.3 DEFINITION OF RCR (%)

The RCR (%) is defined by the percentage ratio of reflected crack number over existing crack number. Although the concept is straightforward, it still needed some clarification before field surveys and data analysis. Figure 3-2 illustrates the RCR concept. In Figure 3-2, the existing crack number (or joint number for Portland cement concrete [PCC]) is 10. After five years, although some cracks propagated in the vertical direction, no crack propagated to the surface, which means no crack could be observed from the surface. Thus, the RCR is still 0 percent. After six years, one crack propagated to the surface, and the RCR becomes 10 percent. If a crack propagated to the surface and could be clearly observed during the survey, it was counted as one reflected crack, regardless of its length or width. Furthermore, if a crack exhibited double or multiple lines, it was still counted as one crack if the lines were less than 5 ft apart.

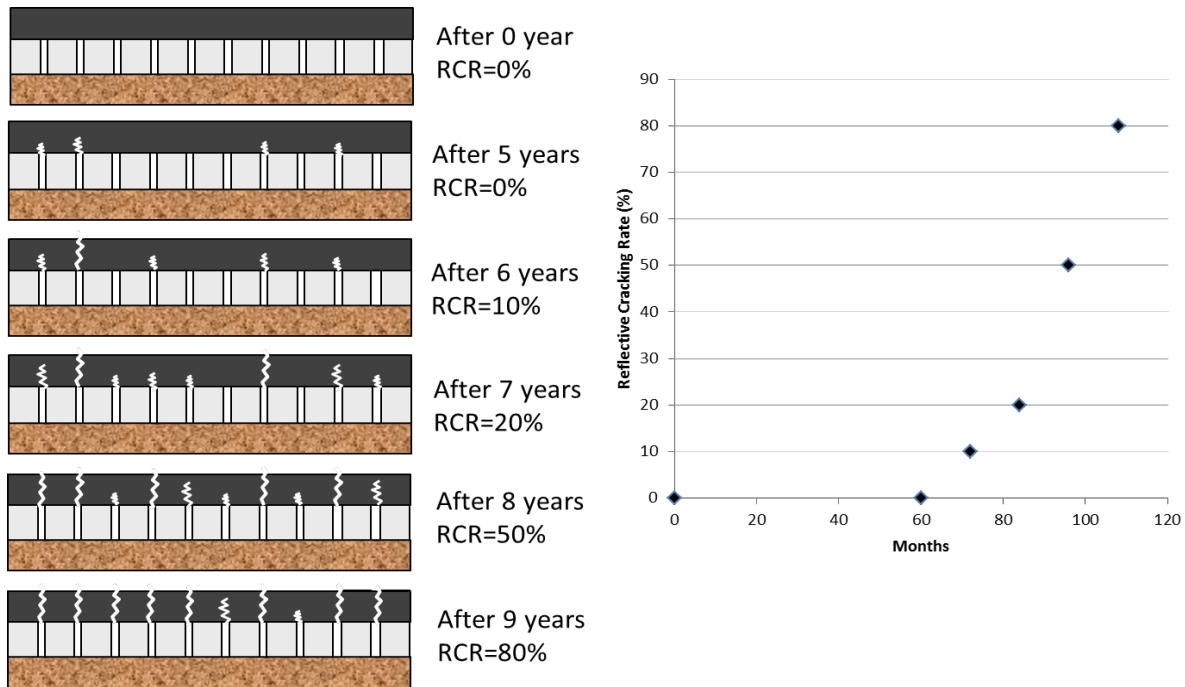


Figure 3-2. RCR Concept.

The following sections present the survey results for each test section. For each test section, the background is briefly introduced, and several representative crack photos (or rut measuring photos) are presented; after that, the total number of reflected cracks and corresponding RCR for each survey are calculated and presented in tables and figures.

3.4 SURVEY RESULTS OF PUMPHREY STREET

A thin (1 inch–1.5 inch) hot-mix asphalt (HMA) overlay was constructed on Pumphrey Street in Fort Worth from July 30, 2007, to August 3, 2007. See Figure 3-3.

Pumphrey Street Overlay Material and Thickness



Figure 3-3. Schematic Diagram of Pumphrey Street Pavement Structure.

Two dense-graded Type F mixes were designed for this project following the new proposed balanced mix design procedure with the Hamburg and Overlay tests. These two mixes had the same original PG 64-22 binder, aggregates, and gradation but different binder modifiers. One

mix was modified with 7 percent crumb rubber (mainly used in the outside lane of the main road), and the other was modified with 3 percent styrene-butadiene rubber (SBR) latex (mainly used in the inside lane of the main road). Figure 3-4 shows the plan view of the main road (southbound and northbound) and ramps (from R1 to R6). A total of eight test sections were surveyed.

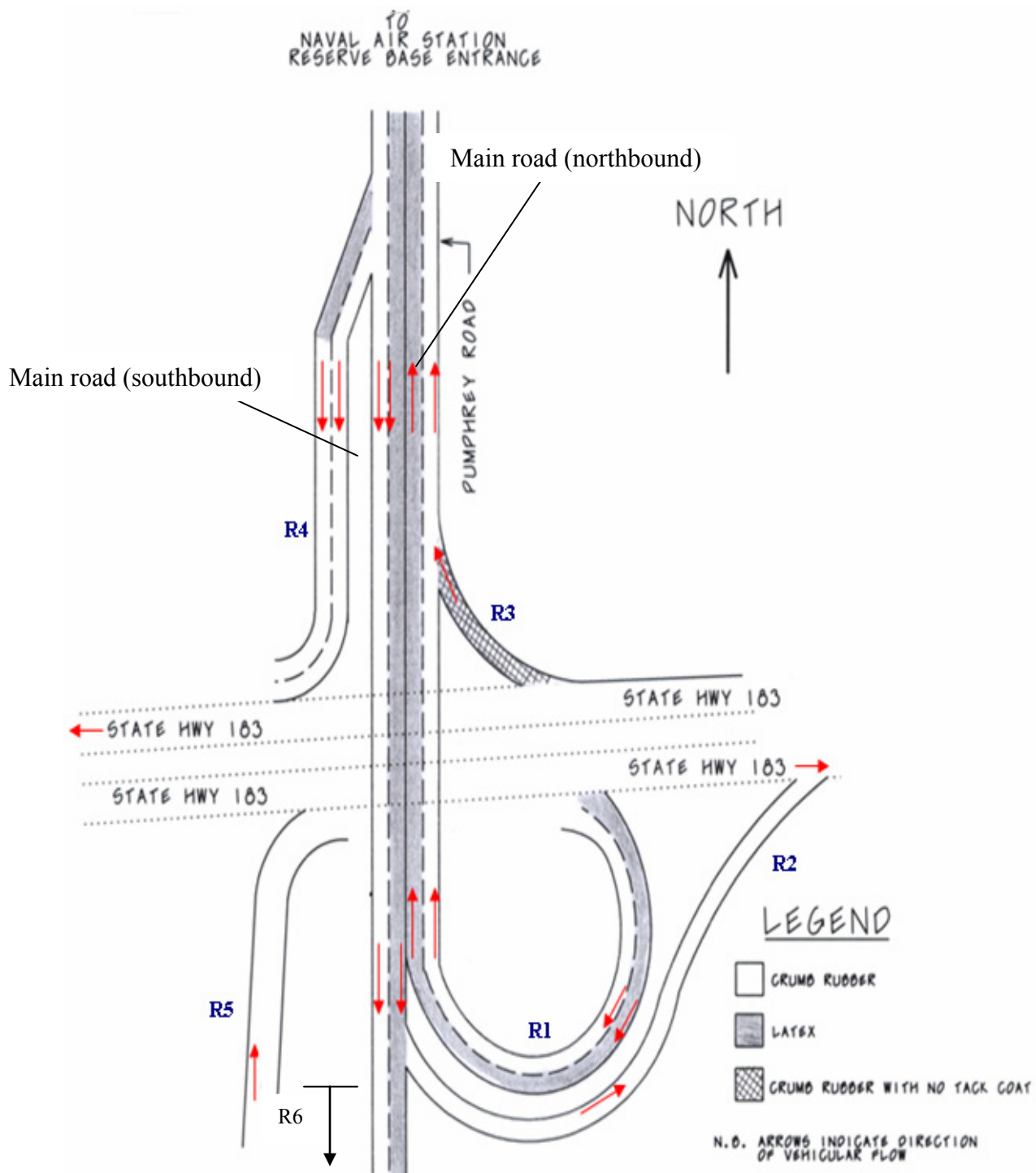


Figure 3-4. Plan View of Pumphrey Street Sections (drawing not to scale).

Figures 3-5 and 3-6 are road photos taken from the overpass.

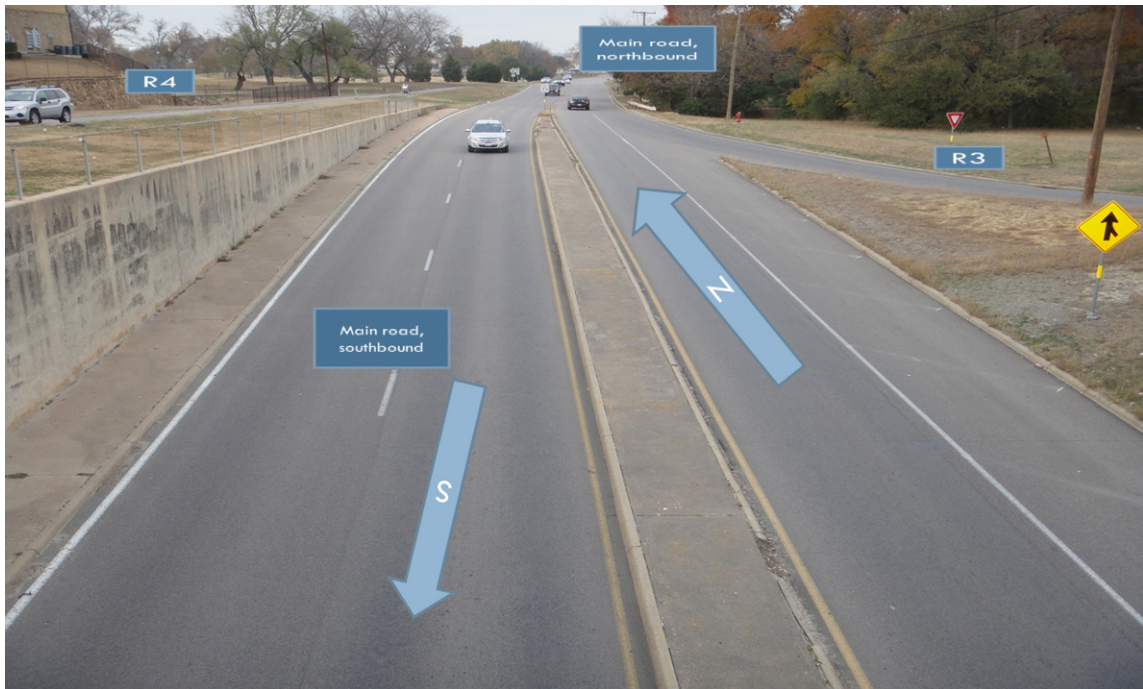


Figure 3-5. Photo of Pumphrey Street Sections (taken from overpass, facing north).



Figure 3-6. Photo of Pumphrey Street Sections (taken from overpass, facing south).

After construction, three visual site inspections on this thin overlay project were conducted on December 14, 2007, April 2, 2008, and July 30, 2008. Few cracks were found in the main road, but some cracks were observed in the ramps at that time. The surveys were conducted before Project 5-5123-03 started, so cracks were not photographed, and no exact crack numbers were counted.

On December 11, 2009, May 7, 2010, September 10, 2010, April 6, 2011, December 9, 2011, and July 19, 2012, six more surveys were conducted, and the cracks were numbered and photographed. No rutting was found during this period.

Figure 3-7 shows the development of the same reflective crack during each survey. These photos reveal that although the crack generally got wider and longer as time passed, during the summer, it diminished due to healing and was thus sometimes hard to find (see Figure 3-7c).

Tables 3-1 and 3-2 present the total crack number information of the Pumphrey Street sections. Since the main road overlays had different mixtures in the outside lane (crumb rubber mixes) and the inside lane (latex mixes), the main road test section (northbound and southbound) are further divided into four sections when summarizing the reflected crack numbers.



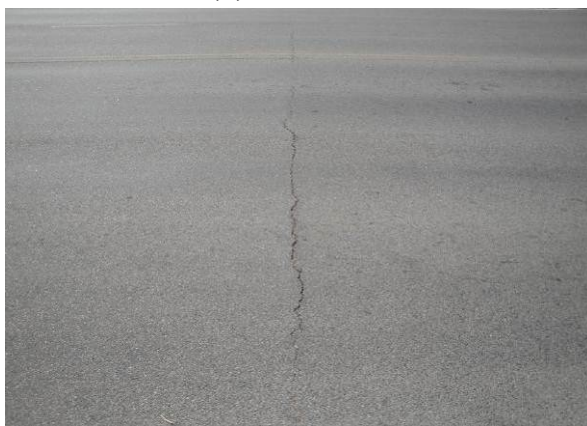
(a) 12/11/2009



(b) 5/7/2010



(c) 9/10/2010



(d) 4/6/2011



(e) 12/09/2011



(f) 7/19/2012

Figure 3-7. Photos of the Same Crack in Pumphrey Street on Each Survey Date.

Table 3-1. Crack Number of Pumphrey Street Main Road Sections.

Crack survey date	Months since construction	Northbound, outside lane	Northbound, inside lane	Southbound, outside lane	Southbound, inside lane
7/30/2008	11	0	0	0	0
12/11/2009	28	16	3	1	1
5/7/2010	33	23	7	8	7
4/6/2011	44	39	12	23	16
12/9/2011	50	42	13	35	21
7/19/2012	57	43	14	50	28

Note: The data from 9/10/2010 were omitted since some cracks could not be found in summer.

Table 3-2. Crack Number of Pumphrey Street Ramp Sections.

Crack survey date	Months Since construction	R1	R2	R3	R4	R5	R6
12/11/2009	28	30	17	9	31	15	12
5/7/2010	33	36	18	11	31	16	12
9/10/2010	37	36	20	12	32	17	12
4/6/2011	44	41	23	14	35	24	12
12/9/2011	50	45	25	14	35	24	12
7/19/2012	57	47	28	16	37	24	12

Because the existing layer was a PCC layer, the total joints for each section could be counted as the existing crack number, and then the RCR was calculated (see Tables 3-3 and 3-4).

Table 3-3. RCR (%) of Pumphrey Street Main Road Sections.

Crack survey date	Months since construction	Northbound, outside lane	Northbound, inside lane	Southbound, outside lane	Southbound, inside lane
7/30/2008	11	0.0	0.0	0	0
12/11/2009	28	11.5	2.2	0.7	0.7
5/7/2010	33	16.5	5.0	5.8	5.0
4/6/2011	44	28.1	8.6	16.5	11.5
12/9/2011	50	30.2	9.4	25.2	15.1
7/19/2012	57	30.9	10.1	36.0	20.1

Note: The data from 9/10/2010 were omitted since some cracks could not be found in summer.

Table 3-4. RCR (%) of Pumphrey Street Ramp Sections.

Crack survey date	Months since construction	R1	R2	R3	R4	R5	R6
12/11/2009	28	54.5	37.8	50.0	70.5	55.6	80.0
5/7/2010	33	65.5	40.0	61.1	70.5	59.3	80.0
9/10/2010	37	65.5	44.4	66.7	72.7	63.0	80.0
4/6/2011	44	74.5	51.1	77.8	79.5	88.9	80.0
12/9/2011	50	81.8	55.6	77.8	79.5	88.9	80.0
7/19/2012	57	85.5	62.2	88.9	84.1	88.9	80.0

Figures 3-8 to 3-9 show the RCR developing curves of the Pumphrey Street sections. These figures show that the RCR on the ramps was much larger than on the main lanes. The reason might be that the existing layer on the main lanes was pre-treated before asphalt overlay, and the LTE at joints was improved. Another finding was that the outside lanes in both directions (southbound and northbound) had higher RCR than the inside lanes, which implies that the latex mix performed better than the crumb rubber mix in terms of cracking resistance.

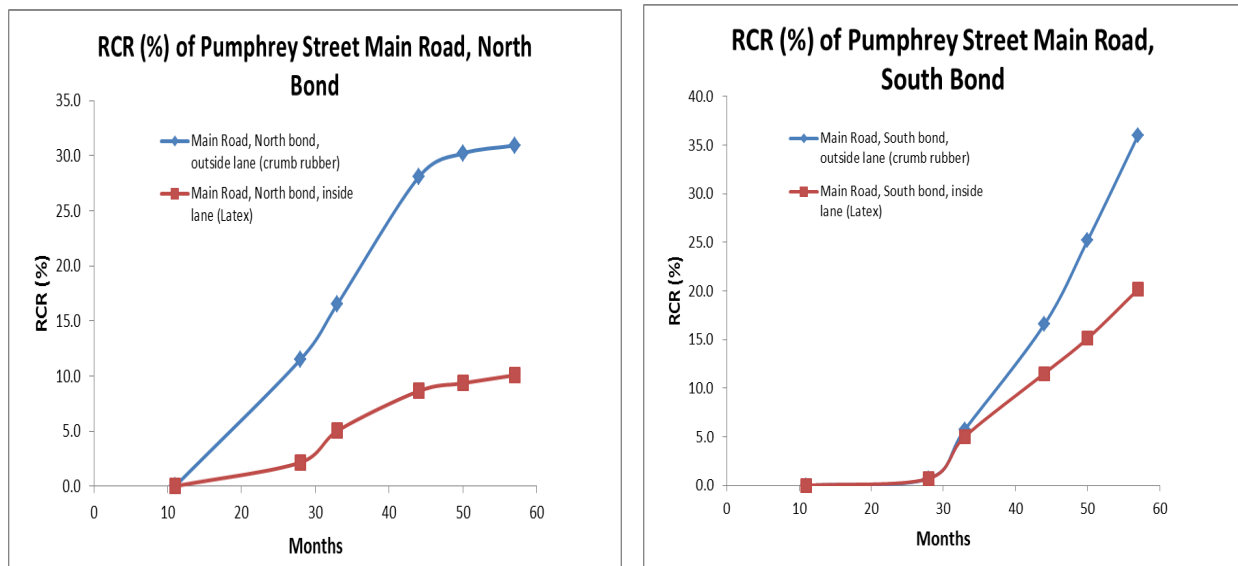


Figure 3-8. RCR vs. Months of Pumphrey Street Main Road Sections.

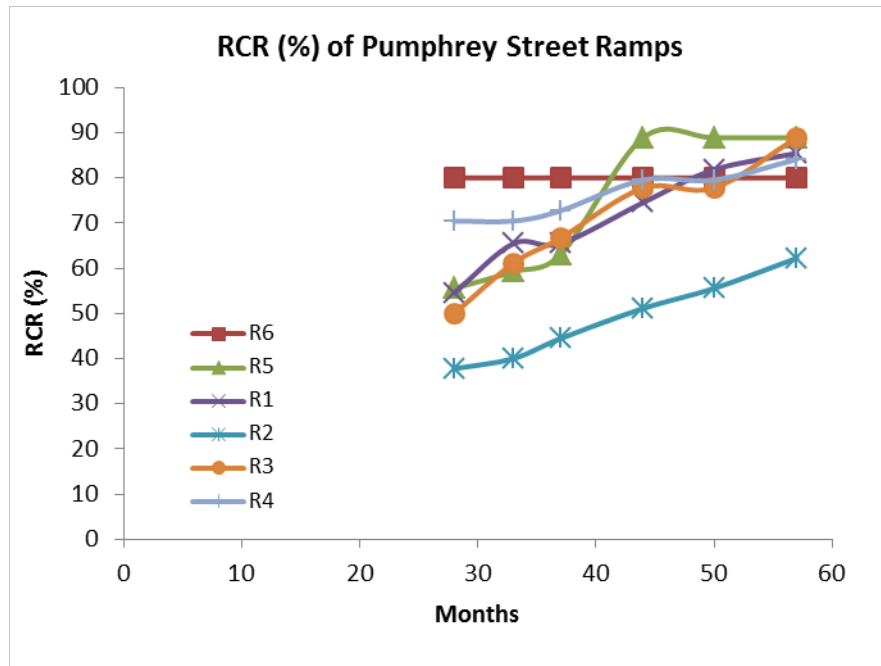


Figure 3-9. RCR vs. Months of Pumphrey Street Ramp Sections.

3.5 SURVEY RESULTS OF SH 12

The overlay section on SH 12 was constructed in September 2006 with 1 inch crack attenuation mix (CAM), 2 inch Type D, and 1.5 inch porous friction concrete (PFC). See Figure 3-10.

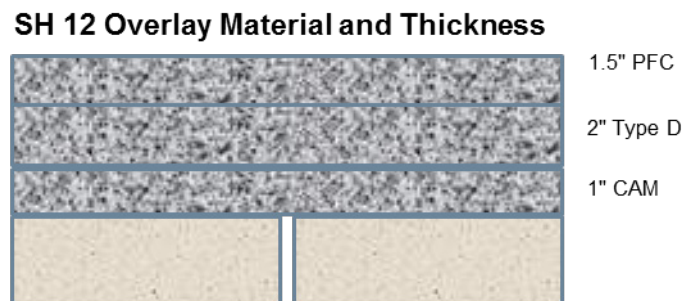


Figure 3-10. Schematic Diagram of SH 12 Pavement Structure.

Figure 3-11 shows the overview of this section.



Figure 3-11. SH 12 Test Section Overview.

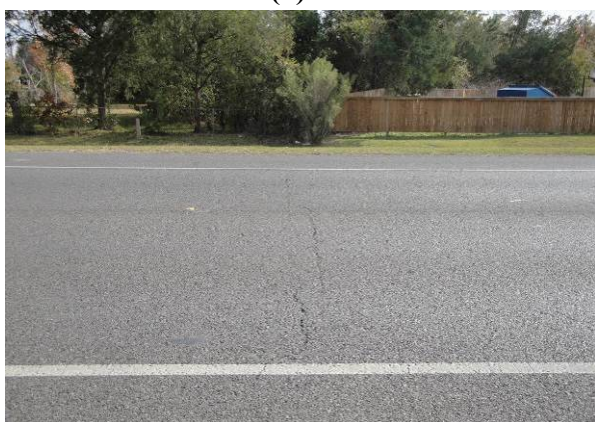
The surveys were conducted on December 9, 2009, April 23, 2010, December 9, 2010, June 2, 2011, October 13, 2011, and May 17, 2012. Figure 3-12 shows the photos of the same crack during each survey on SH 12. All the observed reflective cracks had already been sealed with crack sealant in the spring of 2011.



(a) 12/9/2009



(b) 4/23/2010



(c) 12/9/2010



(d) 6/2/2011



(e) 10/13/2011



(f) 5/17/2012

Figure 3-12. Photos of the Same Crack in SH 12 on Each Survey Date

No rut was found in this section. See Figure 3-13.



Figure 3-13. Rut Measurement on SH 12.

Table 3-5 includes the cracking numbers and RCR during each survey.

Table 3-5. Crack Number and RCR (%) of SH 12 during Each Survey.

Crack survey date	Months since construction	Crack number	RCR (%)
10/4/2007	13	0	0
12/9/2009	39	38	11.0
4/23/2010	43	80	23.1
12/9/2010	51	115	33.2
6/2/2011	57	137	39.6
10/13/2011	61	140	40.5
5/17/2012	68	147	42.5

Note: There was an investigation on 10/4/2007 (before the project 5-5123-03 started) and no crack was found in SH 12 at that time.

Figure 3-14 shows the curve of RCR vs. months.

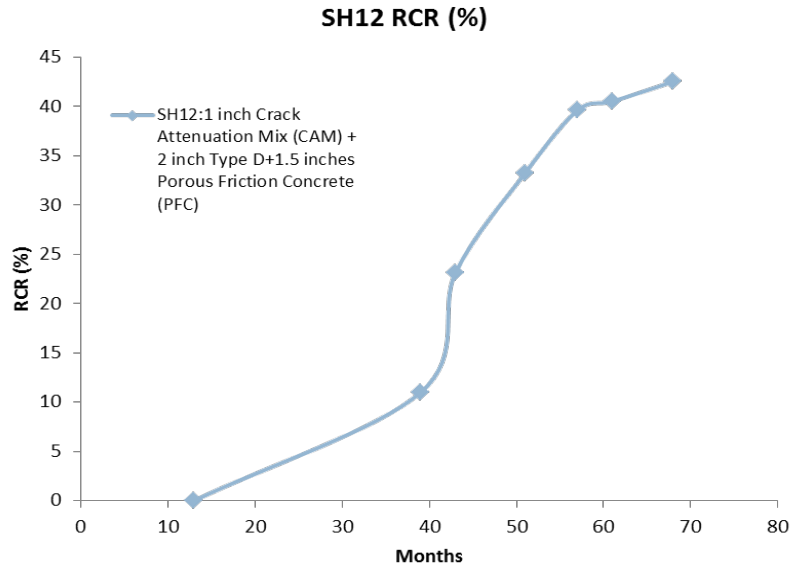


Figure 3-14. SH 12 RCR (%) vs. Months.

3.6 SURVEY RESULTS OF US 82

This section had 8 inch stone mastic asphalt (SMA) overlay and was constructed in 2003.

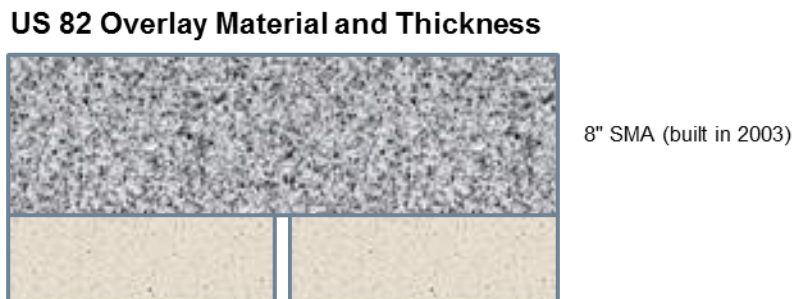


Figure 3-15. Schematic Diagram of US 82 Pavement Structure.

The surveys were conducted on December 17, 2009, April 30, 2010, December 16, 2010, June 17, 2011, December 8, 2011, and July 19, 2012. After 9 years of service under heavy traffic, there were still no cracks observed on the surface. See Figure 3-16.



Figure 3-16. US 82 Overlay Section Overview.

However, in some areas, especially uphill areas, some rutting did exist. See Figure 3-17.



Figure 3-17. US 82 Rut Measurement.

Table 3-6 lists the rut depth development during each survey.

Table 3-6. Rut Depth (mm) of US 82 at Wheel Path during Each Survey.

Location	Rut depth on 06/17/2011 (95 months)	Rut depth on 12/08/2011 (101 months)	Rut depth on 07/19/2012 (108 months)
Location 1 (uphill-1)	8.82	9.93	11.31
Location 2 (uphill-2)	6.59	7.82	8.95
Location 3 (flat area)	2.53	4.02	5.13

3.7 SURVEY RESULTS OF SH 24

The SH 24 test section consisted of a 2.5 inch Type D mix, 3 inch Type B asphalt concrete, 11 inches of cement-treated base, 8 inches of lime treated subgrade, and natural subgrade. See Figure 3-18. The 2.5 inch Type D overlay was constructed in July 2009.

SH 24 Overlay Material and Thickness

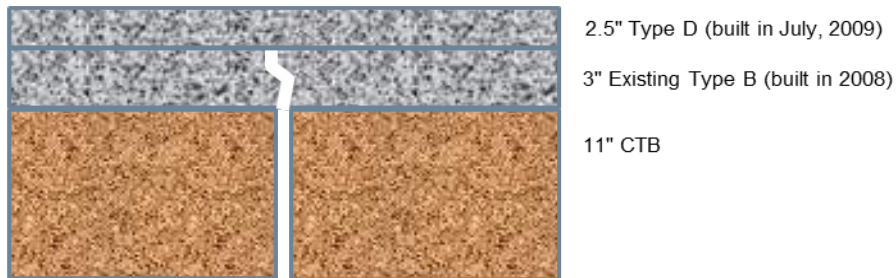


Figure 3-18. Schematic Diagram of SH 24 Pavement Structure.

Figure 3-19 shows the overview of the SH 24 test section.



Figure 3-19. Overview of SH 24 Test Section.

The surveys were conducted on April 29, 2010, December 16, 2010, June 17, 2011, and December 8, 2011. Figure 3-20 shows the photos of the same crack during each survey.

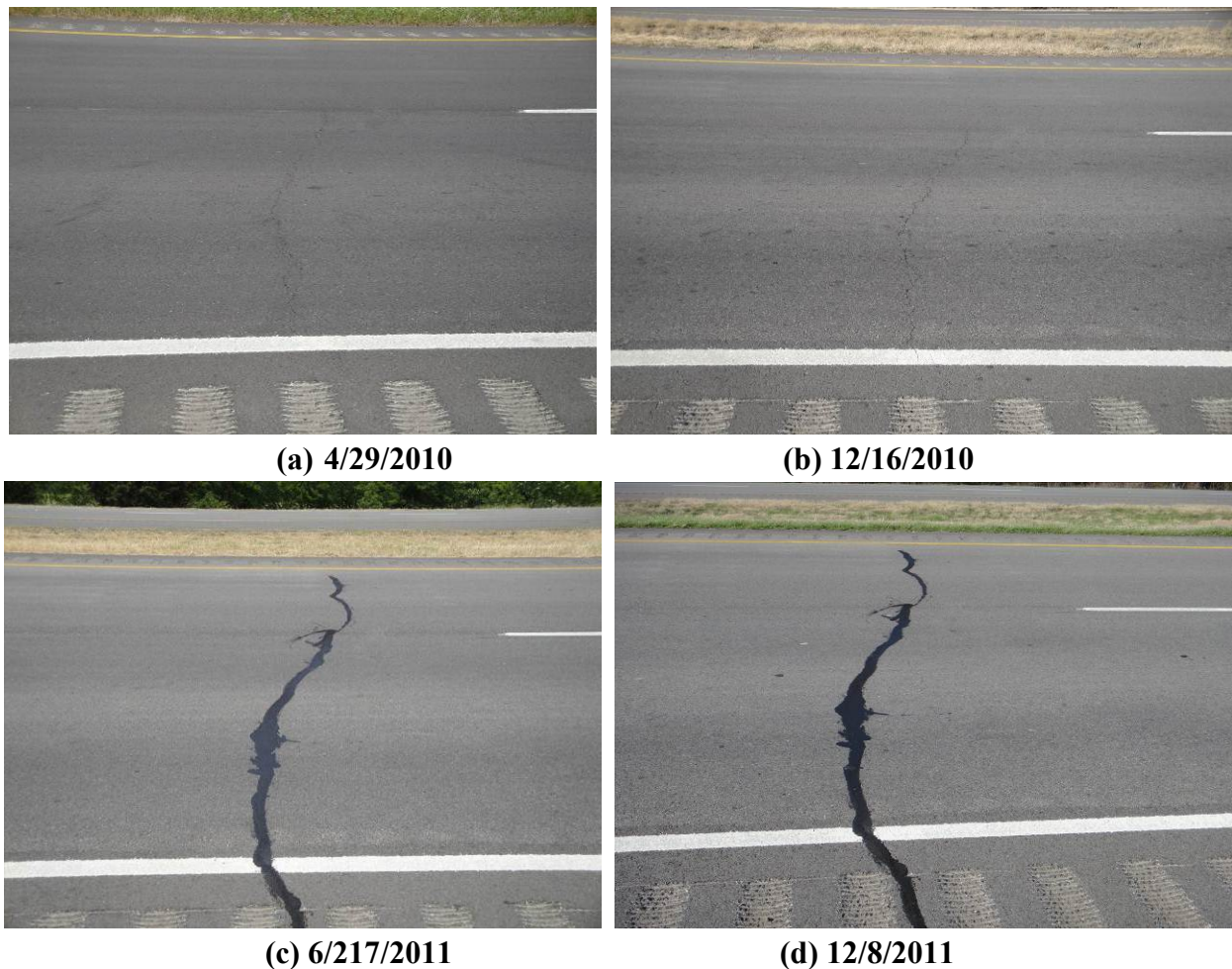


Figure 3-20. Photos of the Same Crack in SH 24 on Each Survey Date.

The cracking numbers during each survey are listed in Table 3-7. No rutting was found in this section.

Table 3-7. Crack Number and RCR (%) of SH 24 during Each Survey.

Crack survey date	Months since construction	Crack number	RCR (%)
4/29/2010	9	26	59.0
12/16/2010	17	32	68.9
6/17/2011	23	54	88.5
12/08/2011	29	57	93.4

Figures 3-21 illustrates the curves of RCR vs. months on SH 24.

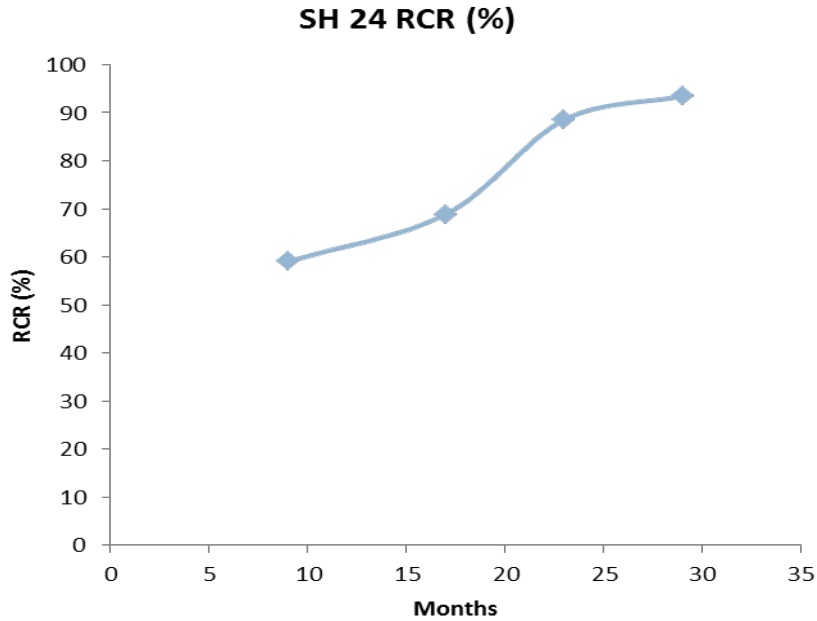


Figure 3-21. SH 24 RCR (%) vs. Months.

3.8 SURVEY RESULTS OF IH 40

Four test sections were constructed in August 2009 on IH 40 eastbound. The overlay mixtures were regular 20% RAP with PG 64-28 binder designed by the contractor (section 0), 0% RAP with PG 64-28 binder designed by the contractor (section 1), 35% RAP with PG 58-28 binder designed by the Texas A&M Transportation Institute (TTI; section 2), and 20% RAP with PG 64-28 binder designed by TTI (section 3). See Figure 3-22.

IH 40 Overlay Material and Thickness

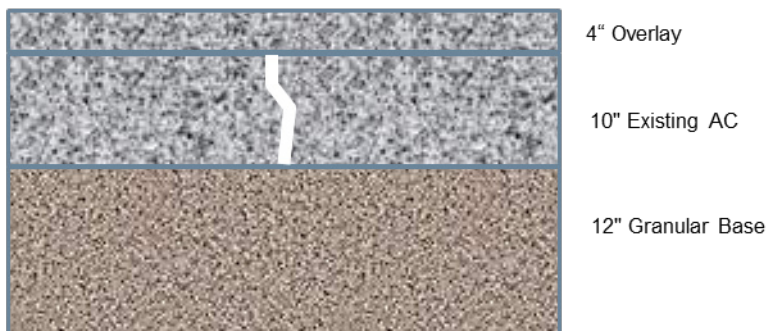


Figure 3-22. Schematic Diagram of IH 40 Pavement Structure.

Figure 3-23 shows the overview of the IH 40 test sections.



Figure 3-23. Overview of IH 40 Test Sections.

The surveys were conducted on April 22, 2010, September 8, 2010, April 5, 2011, December 15, 2011, and May 30, 2012. Figure 3-24 shows the photos of the same crack during each survey. In April 2011, the westbound lanes of IH 40 in this area were under construction, so the eastbound lanes were divided into two directions of traffic, as seen in Figure 3-24(c).



(a) 4/22/2010



(b) 9/8/2010



(c) 4/5/2011



(d) 12/15/2011



(e) 5/30/2012

Figure 3-24. Photos of the Same Crack on IH 40 on Each Survey Date.

The RCR for each test section during each survey was determined and is listed in Table 3-8.

Table 3-8. RCR (%) of IH 40 Test Sections during Each Survey.

	Months since construction	Section 0 (20% RAP—Contractor)	Section 1 (0% RAP—Contractor)	Section 2 (35% RAP—TTI)	Section 3 (20% RAP—TTI)
4/22/2010	8	0.0	0.0	0.0	0.0
9/8/2010	13	36.1	20.0	0.0	4.2
4/5/2011	20	83.3	52.5	28.6	50.0
12/15/2011	28	97.2	65.0	38.1	83.3
5/30/2012	33	97.2	80.0	57.1	95.8

Figure 3-25 shows the curves of RCR vs. months for the IH 40 test sections.

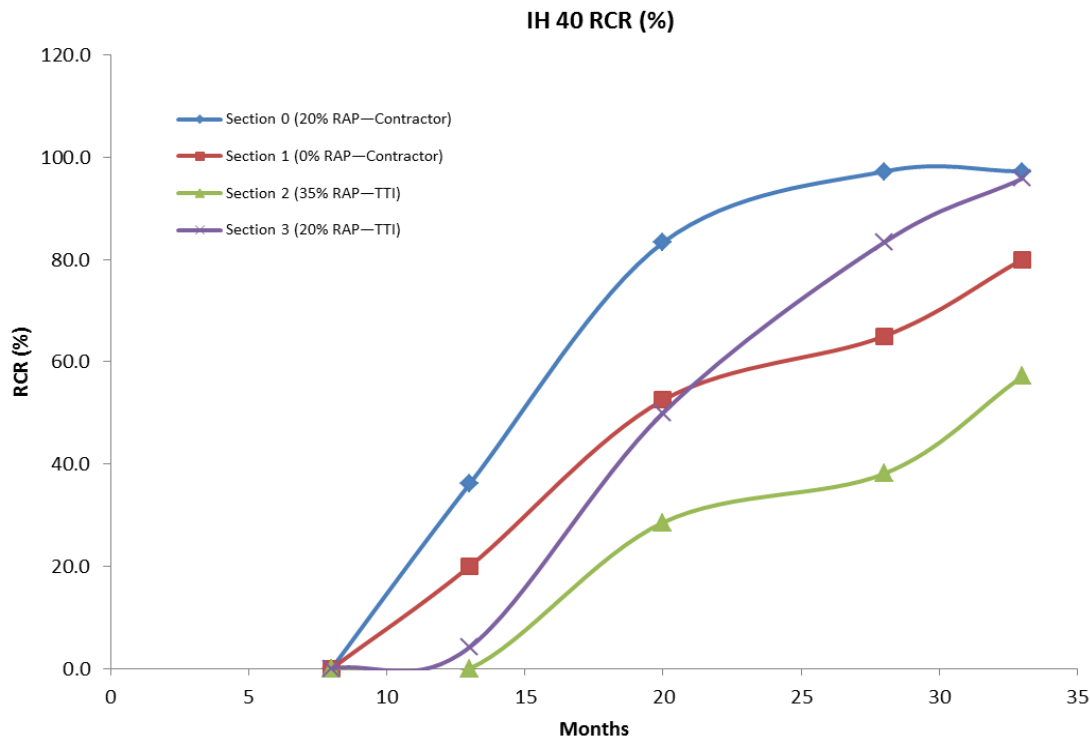


Figure 3-25. RCR vs. Months on IH 40 Test Sections.

3.9 SURVEY RESULTS OF SH 359

An asphalt overlay test section with 20 percent RAP was constructed on SH 359 eastbound in March 2009. The overlay thickness was 3 inches. See Figure 3-26.

SH 359 Overlay Material and Thickness



Figure 3-26. Schematic Diagram of SH 359 Pavement Structure.

Figure 3-27 shows the overview of the SH 359 test section.



Figure 3-27. Overview of SH 359 Test Section.

The surveys were conducted on December 20, 2010, April 11, 2011, December 19, 2011, and May 24, 2012. No cracking or rutting was found during these surveys. See Figure 3-28.



Figure 3-28. No Crack, No Rutting in SH 359 Test Section, as of 5/24/2012.

3.10 SURVEY RESULTS OF US 87

There were two test sections on US 87; one mixture was contractor designed with regular asphalt content, and the other mixture was TTI designed with a higher asphalt content. The overlay thickness was 3 inches and was placed in October 2010. See Figure 3-29.



Figure 3-29. Schematic Diagram of US 87 Pavement Structure.

Figure 3-30 shows the overview of the US 87 test sections.



Figure 3-30. Overview of US 87 Test Sections.

The surveys were conducted on October 20, 2010 (construction date), April 5, 2011, December 15, 2011, and May 30, 2012. In these test sections, the traffic was closed from July 2011 until April 2012. Before April 2012, these test sections functioned as a two-way road, and after that, they functioned as a one-way road since the construction of the other direction of US 87 was finished and opened to traffic.

Figure 3-31 shows the photos of the same crack during each survey. Figure 3-31(a) is the photo taken just after the overlay construction, and the crack in the shoulder implies the location of the existing crack. In Figure 3-31(b), no crack was observed in the overlay lane. In Figure 3-31(c), the shoulder was repaved, but the shoulder crack could still be traced. Figure 3-31(d) clearly shows that the existing crack reflected into the overlay.



(a) 10/20/2010



(b) 4/5/2011



(c) 12/15/2011



(d) 5/30/2012

Figure 3-31. Photos of the Same Crack in US 87 on Each Survey Date.

No rutting was found during these surveys. See Figure 3-32.



Figure 3-32. No Rutting in US 87 Test Sections, as of 5/30/2012.

The RCR for each test section during each survey was determined and is listed in Table 3-9.

Table 3-9. RCR of US 87 Test Sections during Each Survey.

Survey date	Months since construction	Section 1— higher asphalt content	Section 2— regular asphalt content
4/5/2011	6	0.0	0.0
12/15/2011	14	2.9	17.5
5/30/2012	19	17.1	42.5

Figure 3-33 shows the curves of RCR vs. months for US 87 test sections.

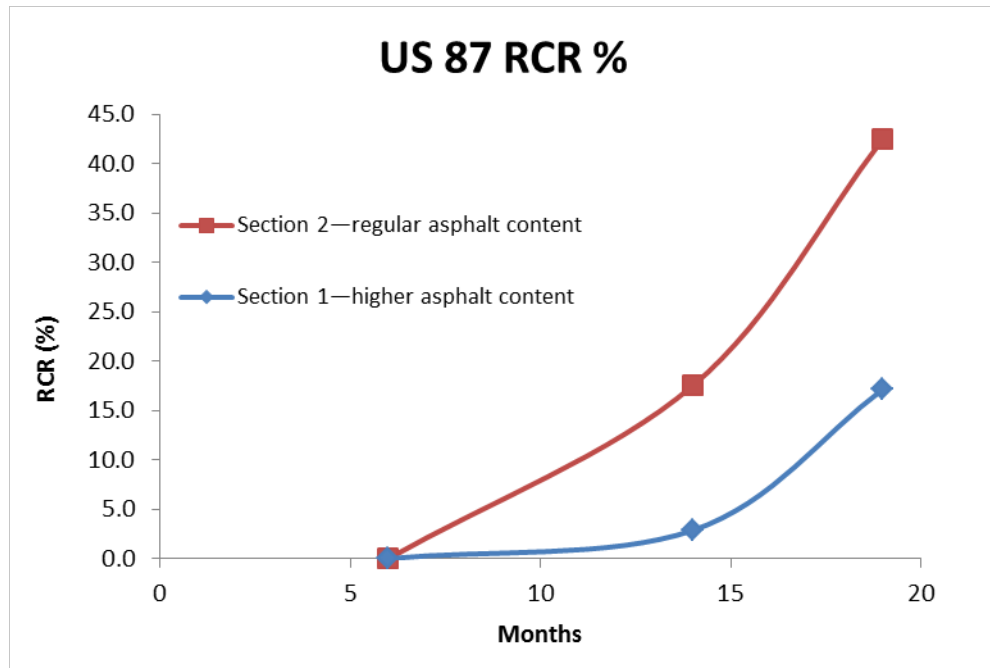


Figure 3-33. RCR vs. Months for US 87 Test Sections.

3.11 SUMMARY

Researchers continuously monitored 18 asphalt overlay test sections in six different districts under Project 5-5123-03. For each survey, the reflected cracks were counted, photographed, and numbered, and the rut depth (if any) was measured. Based on the performance data surveyed in the last four years, several findings were made:

- Either thin or thick asphalt overlays can perform well, depending on existing pavement conditions (e.g., LTE), overlay mix, traffic, and climate. Therefore, asphalt overlay including both mix type and thickness should be designed for project-specific service conditions.
- Asphalt overlay thickness has significant influence on asphalt overlay performance. The overlay thickness has an exponential relationship with asphalt overlay life, so thick overlay is preferred whenever it is possible.
- Overlay mixes with high RAP can be successfully designed to have similar or better performance than virgin mixes provided that the balanced mix design procedure is followed.

- The mix with SBR Latex modified binder performed better than that with crumb rubber modified on Pumphrey Street in Fort Worth.

CHAPTER 4.

DETERMINATION OF KEY INPUT PARAMETERS

Under Project 0-5123, five types of parameters were identified to have significant influence on overlay cracking or rutting performance (*I*), and these key input parameters to the TxACOL are:

- Overlay mixture dynamic modulus, having significant influence on both overlay cracking and rutting performance.
- Overlay mixture cracking property, having significant influence on overlay cracking performance.
- Overlay mixture rutting property, having significant influence on overlay rutting performance.
- Existing layer and subgrade modulus, having significant influence on both overlay cracking and rutting performance.
- LTE of joints/existing cracks, having significant influence on overlay cracking performance.

Among these five types of parameters, the first three are determined by lab testing, and the last two are determined through field falling weight deflectometer (FWD) data analysis. Other factors, such as layer thicknesses and climatic conditions, may also have significant influence on cracking or rutting performance; however, they are beyond the scope of this report.

The following sections discuss the determination of these five types of parameters, one by one, from the TxACOL implementation point of view.

4.1 DYNAMIC MODULUS

The dynamic modulus test (2) is widely accepted by state highway agencies for mechanistic-empirical pavement design. Figure 4-1 shows the test machine and the specimen for the dynamic modulus test. The specimen size is a 4 inch diameter by 6 inch height. Three linear variable differential transformers (LVDTs) are attached on the specimen to measure the strain responses.



Figure 4-1. Dynamic Modulus Test Equipment and Specimen.

The five test temperatures are 14°F, 40°F, 70°F, 100°F, and 130°F, and the six test frequencies are 25 Hz, 10 Hz, 5 Hz, 1 Hz, 0.5 Hz, and 0.1 Hz. Three replicates are often used for the dynamic modulus test. The average dynamic modulus corresponding to each frequency at each temperature is required as input by the TxACOL program. As an example, Table 4-1 lists the dynamic modulus ($|E^*|$) test results.

Table 4-1. Sample $|E^*|$ Values (ksi).

Temperature	Frequency					
	25 Hz	10 Hz	5 Hz	1 Hz	0.5 Hz	0.1 Hz
14°F	2347	2307	2175	1810	1682	1378
40°F	1843	1687	1498	1080	916	619
70°F	820	597	467	280	223	139
100°F	161	118	96	64	54	40
130°F	61	50	43	32	29	23

Figure 4-2 shows the interface of $|E^*|$ inputs in the TxACOL as a Level 1 input.

AC OverLay1

Material Type: **Type D** Thickness(inch): **2.5**

Thermal Coefficient of Expansion (1e-6 in/in/F) **13.5** Poisson Ratio: **0.35**

Superpave PG Binder Grading

High Temp (C)	Low Temp (C)	
	-22	-28
64		
70		
76		

Material Performance Properties

Fracture Properties

Rutting Properties

Modulus Input

☐ Level 3 (Default Value) ☐ Level 2 (Witczak Model) ☒ Level 1 (Test Data)

Test Data

Dynamic Modulus (E*,ksi)

Number of Temperatures: **5** Number of frequencies: **6**

Temperature (F)	Frequency (Hz)					
	25	10	5	1	0.5	0.1
14	2346.7	2307.4	2175	1810	1682	1378
40	1843	1687	1498	1080	916	619
70	820	597	467	280	223	139
100	161	118	96	64	54	40
130	61	50	43	32	29	23

Import **Export**

OK **Cancel**

Figure 4-2. Dynamic Modulus Input Interface.

TxACOL automatically determines the master curve parameters and shift factors corresponding to these dynamic modulus values. Figure 4-3 illustrates the shifted master curve, corresponding equations, and parameters. Based on these determined master curve parameters, δ , α , β , and γ , and shift factor parameters, a , b , and c , TxACOL will calculate the asphalt overlay modulus at any overlay depth, temperature, and vehicle loading frequency. The asphalt layer modulus combined with other layer thickness and modulus is used to predict cracking propagation, reflective cracking development, and the growth of rut depth.

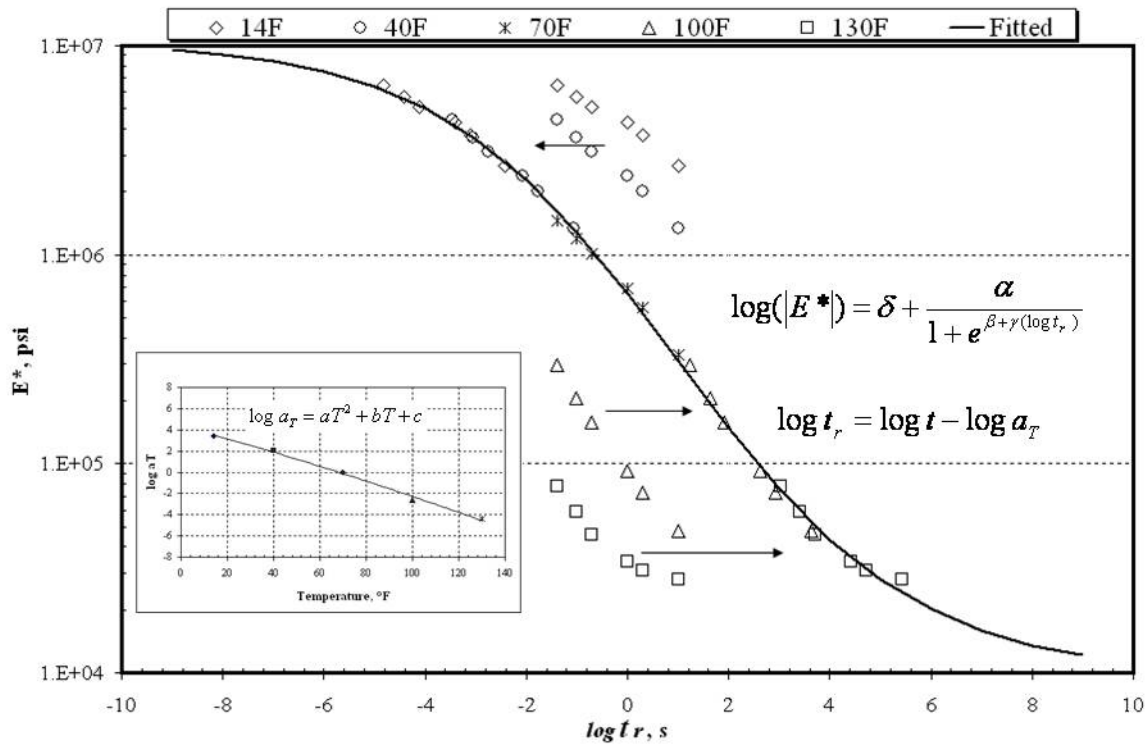


Figure 4-3. Dynamic Modulus Master Curve and Equations.

For the dynamic modulus Level 3 input, users only need to click the Level 3 radio button shown in Figure 4-2, since the default values of δ , α , β , γ , a , b , and c for each selected asphalt overlay mixture (depending on asphalt PG grade and mix type) are already provided in the TxACOL.

Since the regular dynamic modulus test is fairly time consuming and costly, especially the specimen preparation time, in recent years, researchers have recommended using fewer test temperatures or test frequencies to increase test efficiency without compromising accuracy. For example, Bonaquist and Christensen (3) proposed three temperatures (40, 70, and 115°F) and four frequencies (10, 1, 0.1, and 0.01 Hz). Thus in the TxACOL, users should select values from the “number of temperatures” and “number of frequencies” dropdown boxes (Figure 4-2) to adjust the rows and columns of the table. TxACOL has no problem accommodating and processing the dynamic test data like that proposed by Bonaquist and Christensen.

4.2 FRACTURE PROPERTY

The fracture properties A and n are determined by an Overlay test (OT) (4). Based on the recorded maximum load at each cycle, the load reduction, the crack length (c) can be estimated

at each load repetition. Correspondingly, the crack length incremental ΔC (or dc/dN) and SIF value under each load repetition N can be obtained (5).

Figure 4-4 presents the final fitting parameters for dc/dN vs. SIF curve. In this case, $A = 8.9728E-7$, and $n = 4.2061$.

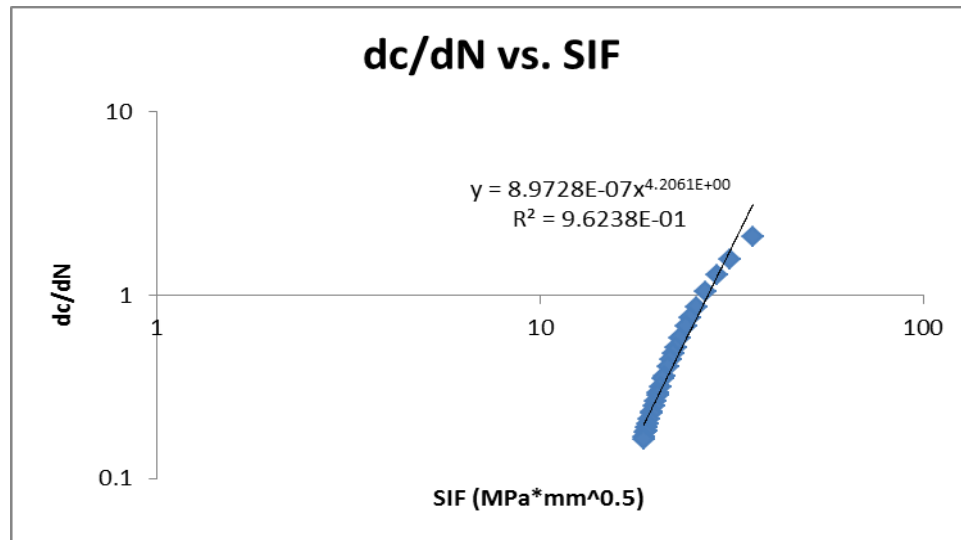
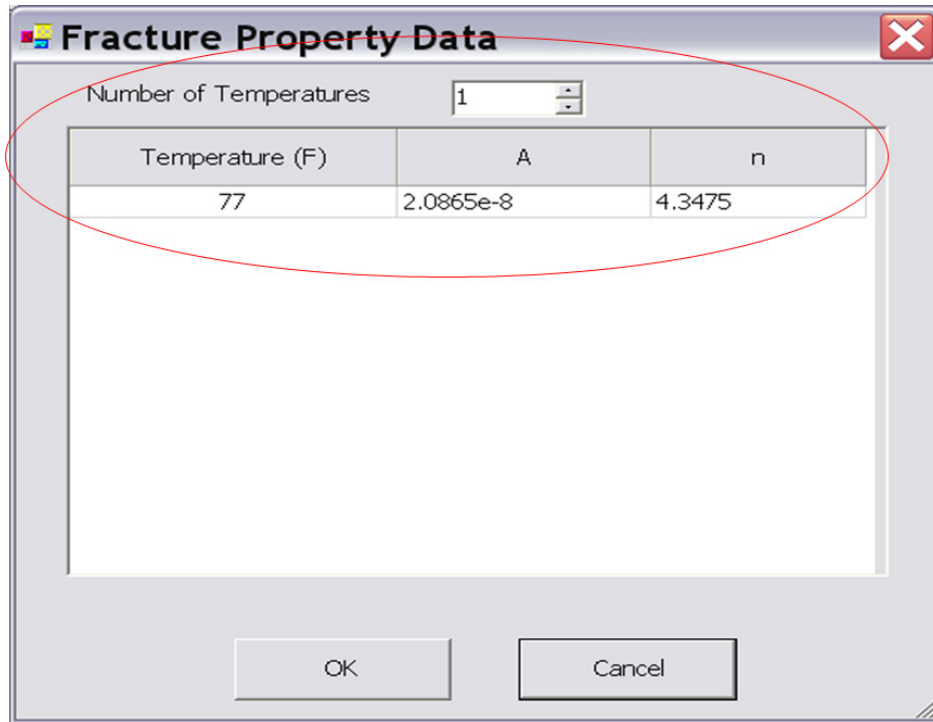


Figure 4-4. A and n Determination.

Figure 4-5 shows the input interface for cracking properties. TxACOL provides the option for multiple cracking property inputs if the OT was conducted under different temperatures.

However, calibration here was conducted based on the A and n values at 77°F alone.

A screenshot of a software dialog box titled "Fracture Property Data". The dialog has a standard Windows-style title bar with a close button (X) in the top right corner. Inside the dialog, there is a label "Number of Temperatures" followed by a spin box containing the value "1". Below this is a table with three columns: "Temperature (F)", "A", and "n". The first row of the table contains the values "77", "2.0865e-8", and "4.3475". The table is enclosed in a red oval. At the bottom of the dialog, there are two buttons: "OK" and "Cancel".

Temperature (F)	A	n
77	2.0865e-8	4.3475

Figure 4-5. A and n Input Interface.

It is recommended to test five replicates to determine the cracking property. To simplify the process of determining reasonable A and n values, the research team developed a new tool to handle multiple OT data files and automatically determine the A and n values based on the OT files. Users can select single or multiple files by checking/unchecking the checkbox shown in Figure 4.6. Figure 4-7 presents the output of the analysis result.

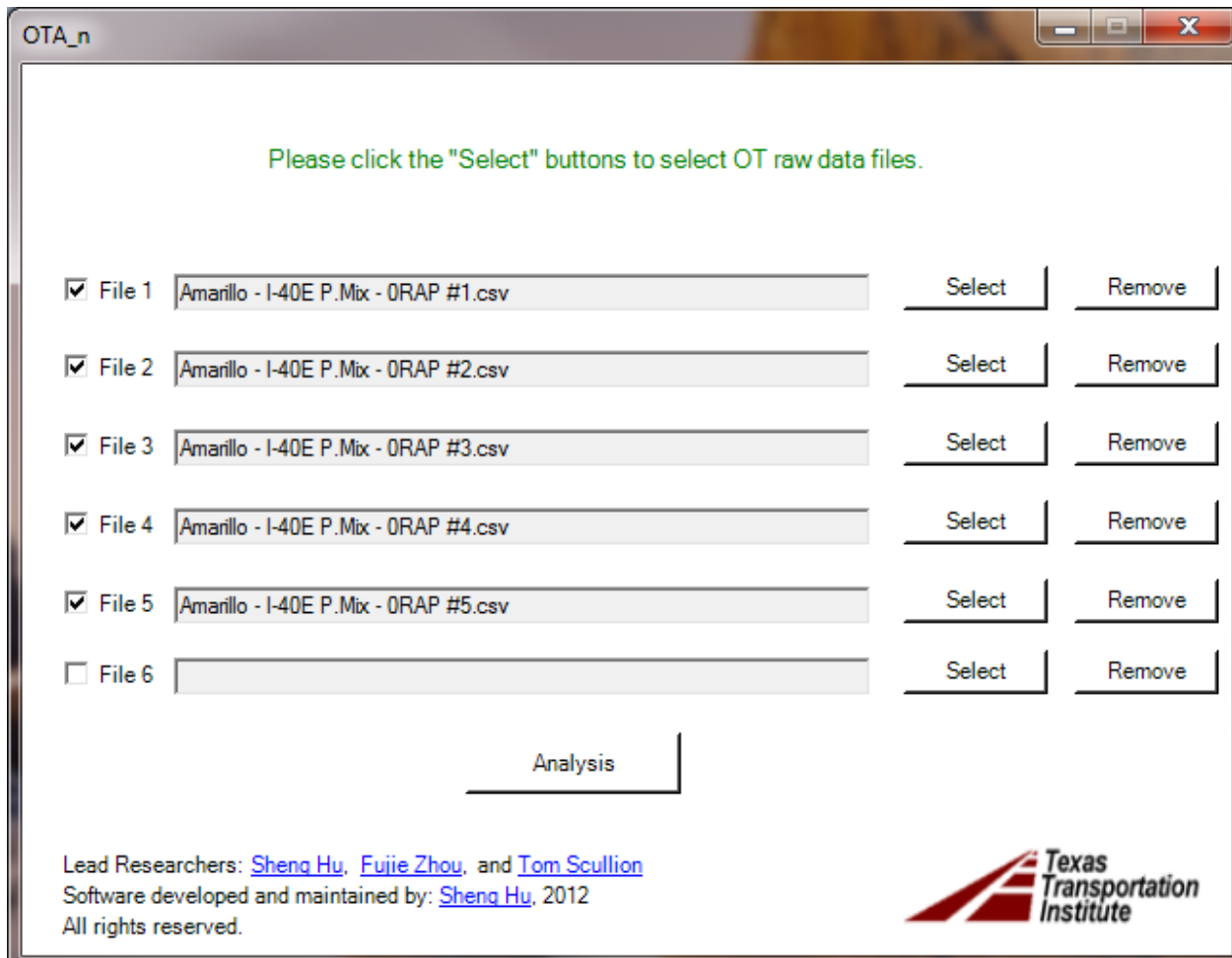


Figure 4-6. Interface of A and n Analysis Tool with Multiple OT Data File Handling.

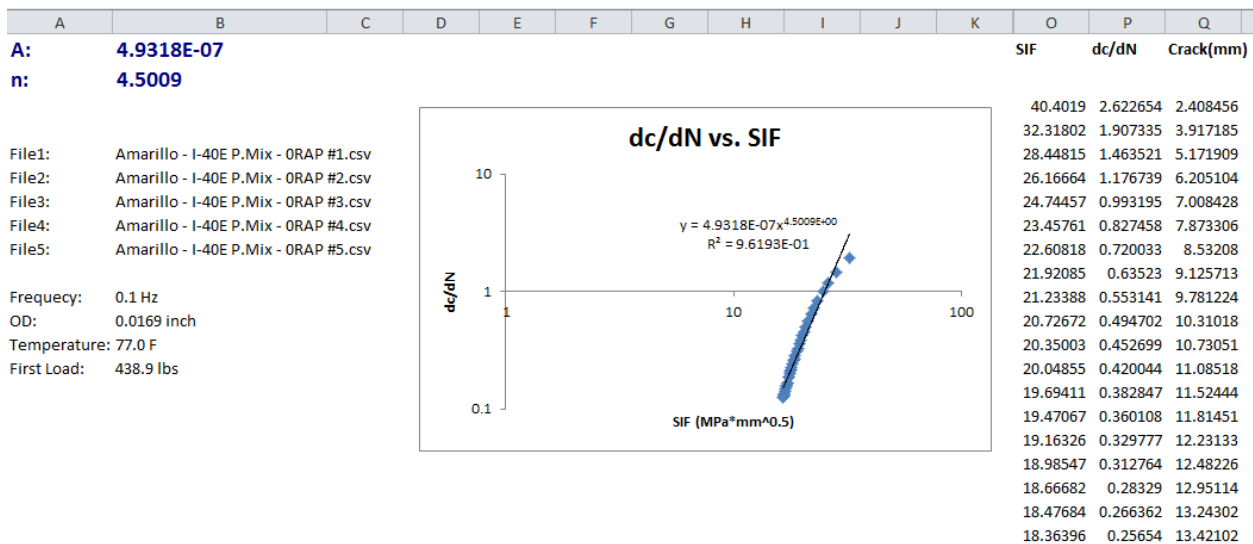
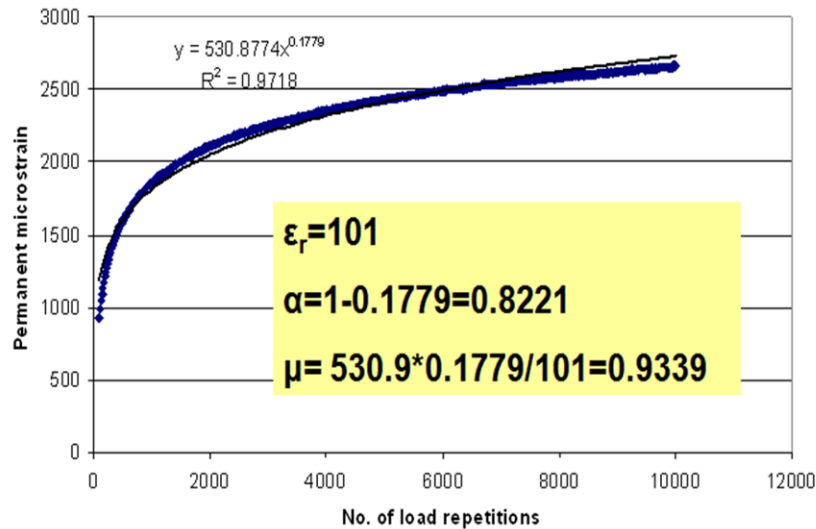


Figure 4-7. Output of the OT A and n Analysis Tool.

4.3 RUTTING PROPERTY

A repeated load test is required to determine the rutting properties α and μ (I). The test equipment and the specimen can be the same as in the dynamic modulus test. Two replicates are recommended. The maximum load repetition number is 10,000. Each load repetition time is 0.1 second of loading plus 0.9 second of rest.

Figure 4-8 shows the curve of permanent microstrain vs. number of load repetitions. The determination method of rutting properties α and μ is illustrated in this figure as well. Note that in Figure 4-8, ϵ_r is resilient microstrain; the curve fitting parameters a and b are 530.877 and 0.1779, respectively.



$$\mu = \frac{ab}{\epsilon_r}$$

$$\alpha = 1 - b$$

Figure 4-8. Permanent Micro Strain vs. Number of Load Repetition.

Figure 4-9 shows the input interface for rutting properties. Similar to the input of cracking properties, TxACOL provides the option for multiple rutting property inputs if the repeated load test is conducted at different temperatures. Currently, the test temperature for the repeated load test is preferred to be 104°F.

Number of Temperatures: 1

Temperature (F)	alpha	mu
104	0.7609	0.7265

OK Cancel

Figure 4-9. Rutting Property Input Interface.

The researchers also developed an Excel macro to automatically process the repeated load test data and determine the rutting properties α and μ . See Figure 4.10. For two replicates, researchers recommend determining α and μ for each replicate and then averaging α and μ , respectively.

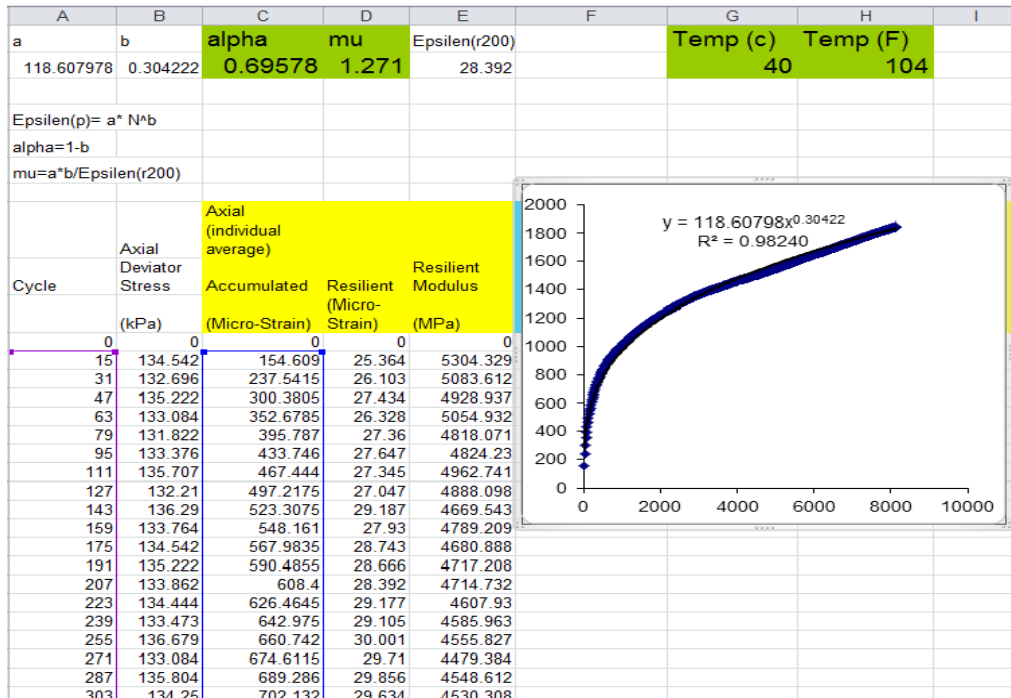


Figure 4-10. Excel Macro for Determining Rutting Properties.

4.4 FWD MODULUS

In Texas, *Modulus 6.0* (6) is commonly used for modulus back-calculation based on FWD data. To enhance the accuracy of modulus back-calculation results, the FWD test data should be checked visually, and the shape of the deflection basin should be examined. Test data where the shape of the deflection basin was irregular should be eliminated from further consideration. Figures 4-11 and 4-12 present examples of regular and irregular deflection basins.

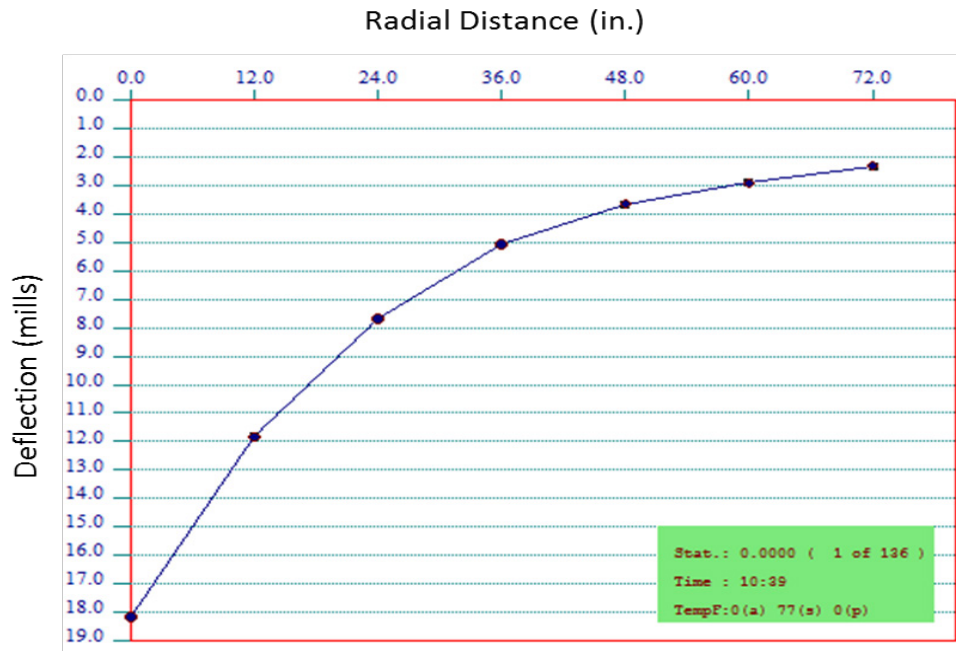


Figure 4-11. An Example of Regular Deflection Basin.

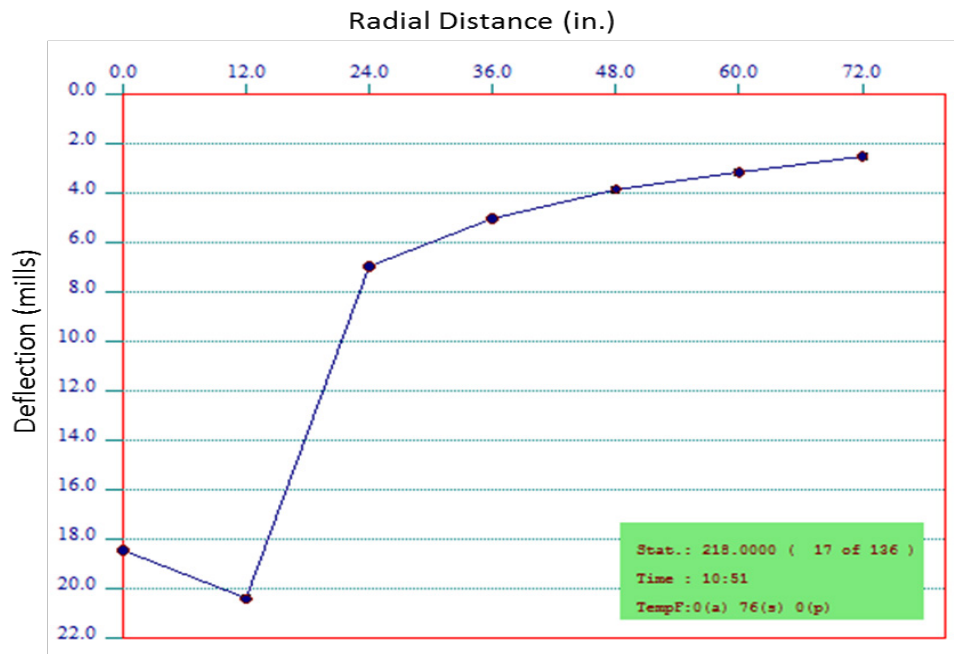


Figure 4-12. An Example of Irregular Deflection Basin.

Figure 4-13 shows an example of a Modulus 6.0 back-calculation result. The mean value then can be used as the input of TxACOL. See Figure 4-14.

TTI MODULUS ANALYSIS SYSTEM (SUMMARY REPORT)														(Version 6.0)	
District:20 (Beaumont) County :122 (JASPER) Highway/Road: US0096				Pavement: Base: 10.00 Subbase: 0.00 Subgrade: 97.98(by DB)				Thickness(in) Minimum 340,000 Maximum 5,700,000 5,000				MODULI RANGE(psi) H1: v = 0.20 H2: v = 0.35 H3: v = 0.00 H4: v = 0.35			
Station	Load (lbs)	Measured Deflection (mil): R1	R2	R3	R4	R5	R6	R7	Calculated Moduli values (ksi): SURF(E1) BASE(E2) SUBB(E3)			SUBG(E4)	Absolute Dpth to Bedrock	ERR/Sens	
0.000	11,070	4.55	4.01	3.55	3.00	2.52	1.96	1.59	3457.9	315.2	0.0	10.8	1.20	147.5	
0.197	11,098	3.63	3.18	2.80	2.27	1.87	1.46	1.17	5165.5	163.8	0.0	16.0	0.92	137.0	
0.399	11,051	4.20	3.72	3.25	2.65	2.21	1.80	1.42	3383.0	340.2	0.0	12.4	0.75	130.4	
0.595	11,035	7.87	7.20	6.61	5.60	4.69	3.57	2.70	3037.8	81.1	0.0	5.8	2.53	125.1	
0.797	10,880	5.10	4.41	3.86	3.12	2.54	1.95	1.50	3324.7	114.5	0.0	11.9	1.01	123.3	
0.994	10,943	4.64	4.18	3.78	3.16	2.68	2.01	1.49	5458.4	59.1	0.0	10.8	1.96	102.6	
1.200	10,975	6.05	5.27	4.56	3.61	2.76	1.89	1.20	2825.1	13.6	0.0	13.6	2.77	81.5 *	
1.393	11,154	2.85	2.35	1.94	1.52	1.20	0.86	0.67	3437.5	316.6	0.0	28.1	1.11	91.5	
1.601	10,876	4.72	4.09	3.54	2.91	2.37	1.80	1.34	3609.0	125.2	0.0	12.8	0.97	104.2	
1.798	11,074	4.40	4.11	3.96	3.35	2.89	2.24	1.69	5500.0	71.7	0.0	10.4	5.29	108.7 *	
1.995	10,979	3.49	3.04	2.66	2.26	1.92	1.56	1.28	3816.0	550.0	0.0	13.5	0.52	145.0	
2.197	10,864	4.88	4.12	3.60	2.68	2.11	1.59	1.09	2649.9	103.6	0.0	15.3	1.46	92.3	
2.399	11,051	3.67	3.24	2.89	2.39	2.03	1.61	1.24	4262.8	401.1	0.0	13.3	1.04	111.1	
2.588	10,721	4.50	4.02	3.60	3.04	2.40	1.91	1.43	5065.9	60.5	0.0	11.8	1.39	103.7	
2.789	10,947	2.69	2.17	1.78	1.36	1.06	0.74	0.59	3183.2	318.3	0.0	32.0	1.47	84.6	
2.999	10,832	4.28	3.81	3.36	2.72	2.24	1.73	1.44	4323.0	131.4	0.0	13.0	1.04	149.4	
3.200	10,947	2.44	2.03	1.64	1.22	0.93	0.66	0.52	4492.1	149.8	0.0	37.8	0.83	88.9	
3.401	11,066	2.41	2.00	1.69	1.29	0.98	0.83	0.68	5500.0	82.2	0.0	36.6	3.86	300.0 *	
3.610	11,039	2.97	2.39	2.01	1.52	1.17	0.84	0.62	3135.3	267.4	0.0	28.8	1.44	95.6	
3.812	10,900	3.16	2.43	1.78	1.31	0.98	0.70	0.50	1743.7	289.0	0.0	35.5	1.48	86.9	
3.996	11,051	1.79	1.41	1.13	0.80	0.58	0.39	0.31	5304.9	148.2	0.0	64.4	1.46	73.5	
4.000	10,939	3.06	2.66	2.30	1.72	1.42	1.01	0.81	5500.0	27.2	0.0	26.9	2.19	96.4 *	
4.194	10,943	2.55	2.21	1.83	1.55	1.22	0.99	0.85	4423.2	547.7	0.0	23.3	0.99	300.0	
4.399	10,892	3.08	2.66	2.30	1.74	1.41	1.03	0.73	5500.0	31.5	0.0	26.1	1.84	89.1 *	
4.600	10,880	2.70	2.30	1.99	1.65	1.34	1.06	0.87	4273.2	550.0	0.0	21.1	0.50	138.1 *	
4.801	10,983	3.06	2.61	2.30	1.90	1.56	1.30	1.10	4096.2	550.0	0.0	17.3	1.22	300.0 *	
4.998	10,876	2.80	2.26	1.98	1.52	1.17	0.90	0.75	3419.0	363.8	0.0	26.5	1.48	130.8	
5.199	10,816	2.99	2.57	2.11	1.79	1.41	1.17	0.95	5500.0	103.0	0.0	22.4	2.83	149.6 *	
5.400	10,896	3.28	2.91	2.48	1.95	1.64	1.30	1.08	4512.2	259.3	0.0	18.0	1.34	168.8	
5.602	10,991	2.20	1.85	1.56	1.24	1.05	0.81	0.69	5500.0	144.2	0.0	36.5	6.64	118.9 *	
5.799	10,717	2.87	2.49	2.15	1.79	1.62	1.11	0.85	4369.7	517.6	0.0	18.2	2.95	300.0	
6.000	10,689	3.24	2.89	2.49	2.01	1.59	1.29	0.99	5161.6	176.3	0.0	18.0	1.00	109.2	
6.204	10,705	3.24	2.69	2.35	1.90	1.51	1.16	0.96	3345.8	364.2	0.0	19.4	1.18	129.3	
6.401	10,816	3.76	3.24	2.83	2.30	1.91	1.41	1.09	4500.3	152.8	0.0	16.1	1.62	109.5	
Mean:		3.62	3.13	2.73	2.20	1.79	1.37	1.06	4199.3	232.1	0.0	21.3	1.77	118.0	
Std. Dev:		1.21	1.14	1.08	0.93	0.79	0.61	0.45	1017.8	169.7	0.0	11.6	1.31	36.3	
Var Coeff(%)		33.41	36.37	39.42	42.28	44.08	44.39	42.60	24.2	73.1	0.0	54.2	73.72	30.7	

Figure 4-13. An Example of Back-Calculation Result.

Existing AC

Material Type: Existing AC Thickness(Inch): 8

Thermal Coefficient of Expansion (1e-6 in/in/F): 13.5 Poisson Ratio: 0.35

Main Cracking Pattern

Cracking Type

☐ Alligator Cracking
 ☐ Longitudinal Cracking
 ☒ Transverse Cracking
 ☐ Block Cracking

Transverse Cracking Options

☒ Severity Level
 Crack Spacing (ft): 15

Severity Level

☐ Low
 ☒ Medium
 ☐ High

FWD Backcalculated Modulus

No. of Temperatures 1

Temperature(°F)	Modulus(ksi)
77	232

OK Cancel

Figure 4-14. FWD Back-Calculated Modulus Input Interface.

4.5 LTE

When the FWD load is applied on the center of a slab and on one side of an existing crack or joint (Figure 4-15), the FWD data can be used to determine the LTE value.



Figure 4-15. FWD Test with the Loading Plate at One Side of Crack.

Researchers used the following equation to determine the LTE value for the existing pavement:

$$LTE = (W_{2j}/W_{1j}) / (W_{2c}/W_{1c}) \quad (4-1)$$

where

W_{1c} = deflection value of sensor 1 when the load is applied on the slab center.

W_{2c} = deflection value of sensor 2 when the load is applied on the slab center.

W_{1j} = deflection value of sensor 1 when the load is applied on the joint.

W_{2j} = deflection value of sensor 2 when the load is applied on the joint.

Figure 4.16 presents the schematic diagram of the relative location of W_{1c} , W_{2c} , W_{1j} , and W_{2j} .

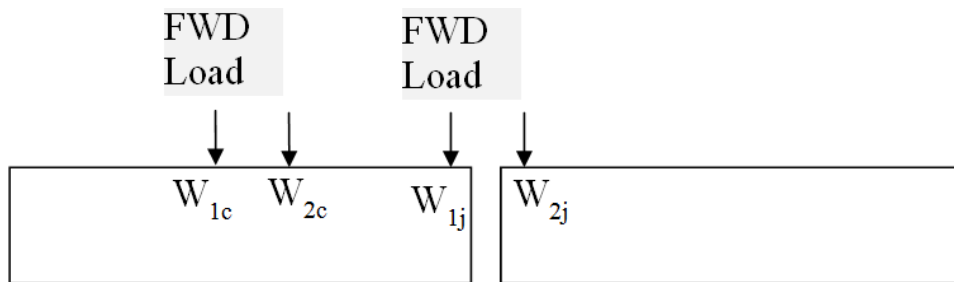


Figure 4-16. Schematic Diagram of W_{1c} , W_{2c} , W_{1j} , and W_{2j} .

According to this LTE determination method, the FWD load should be applied twice to get one LTE value for one crack: one is at the center of the slab, and the other is at the edge of the slab

(or at one side of the crack/joint). Figure 4.17 illustrates the LTE values determined based on an example of FWD data.

		Load	Measured	Deflection (mils):			
		Station	(lbs)	R1	R2	R1/R2	LTE (%)
1/2	Center	0	10,359	9.45	4.15	0.439153	
	Crack	21	10,284	10.03	3.79	0.377866	86
3	Center	67	10,355	7.31	3.55	0.485636	
	Crack	84	10,312	10.31	3.68	0.356935	73
4	Center	99	10,244	6.56	3.34	0.509146	
	Crack	112	10,189	10.49	4.34	0.413727	81
5	Center	136	9,795	9.04	5.14	0.568584	
	Crack	153	10,288	11.52	4.41	0.382813	67
6	Center	169	10,300	8.48	4.07	0.479953	
	Crack	182	10,395	6.36	3.77	0.592767	124
7	Center	196	10,153	10.19	5.63	0.552502	
	Crack	207	10,343	8.87	4.35	0.490417	89
8	Center	222	10,228	9.73	5.33	0.547779	
	Crack	231	10,113	11.72	4.2	0.358362	65
9	Center	248	10,077	11.04	5.7	0.516304	
	Crack	262	10,153	10.57	4.39	0.415326	80
10	Center	290	10,145	7.09	3.41	0.480959	
	Crack	304	10,161	8.3	3.78	0.455422	95
11	Center	325	10,252	6.8	3.82	0.561765	
	Crack	338	10,220	10.49	4.42	0.421354	75
12	Center	351	10,276	3.81	3.01	0.790026	
	Crack	361	10,125	13.41	4.67	0.348248	44
13	Center	373	10,220	4.08	2.91	0.713235	
	Crack	383	10,101	10.63	4.5	0.42333	59
14	Center	405	10,010	10.61	4.92	0.463713	
	Crack	420	10,069	12.74	5.07	0.397959	86
15	Center	440	10,220	3.33	2.72	0.816817	
	Crack	451	10,165	4.68	2.94	0.628205	77

Figure 4-17. LTE Determination Based on FWD Data.

Figure 4-18 shows the LTE input in the TxACOL. Not only the LTE mean value but also the standard deviation of LTE is required.

Existing JPCP(JRCP)

Material Type: Existing JPCP

Thickness(inch): 8 Poisson Ratio: 0.15

Thermal Coefficient of Expansion (1e-6 in/in/F): 5.5

General Properties

Joint/Crack Spacing (ft): 15

Modulus (ksi): 4000

Load Transfer Efficiency (LTE) (%): 70

LTE Standard Deviation: 10

OK Cancel

Figure 4-18. LTE Input Interface.

4.6 DEFAULT VALUES

As mentioned in Chapter 2, the researchers assisted six districts with mix design and mix characterization under Project 5-5123-03. Based on these data, the researchers refined the existing default values for some mixtures, and the refined default values for overlay mixes are listed in Table 4-2. These default values include dynamic modulus master curve parameters, shift factors, fracture properties, and rutting properties. These values are already incorporated into the TxACOL program.

Table 4-2. Default Values.

Binder PG	Mix Type	E* Master Curve Parameters				Shift Factors			Cracking Properties			Rutting Properties	
		δ	α	β	γ	a	b	c	A	n		alpha	mu
6422	Type C	1.510369	2.94191	-0.81681	0.452473	0.00035	-0.12521	7.04985	5.2041E-06	3.8948		0.7315	0.7234
7022	Type C	1.730189	2.74069	-0.79394	0.457858	0.000241	-0.10631	6.25924	5.5095E-06	3.8792		0.7423	0.7014
7622	Type C	1.826459	2.6491	-0.83216	0.459166	0.000219	-0.10016	5.93751	5.8430E-06	3.8630		0.7485	0.6756
6428	Type C	1.401129	3.08811	-0.70145	0.432909	0.000323	-0.11566	6.51138	2.8039E-06	4.0645		0.7315	0.7306
7028	Type C	1.603519	2.90952	-0.6749	0.433476	0.000229	-0.09998	5.87436	3.3231E-06	4.0179		0.7423	0.6986
6422	Type D	1.521429	2.90579	-0.8074	0.45437	0.000353	-0.12568	7.06576	4.2081E-06	3.9531		0.7465	0.8102
7022	Type D	1.741009	2.70536	-0.78165	0.459475	0.000242	-0.10643	6.26374	4.4280E-06	3.9391		0.7521	0.7792
7622	Type D	1.834929	2.61634	-0.81923	0.460231	0.00022	-0.10038	5.94666	4.6659E-06	3.9248		0.7609	0.7265
6428	Type D	1.421189	3.04079	-0.6915	0.436451	0.000328	-0.1163	6.53531	2.4914E-06	4.0969		0.7465	0.8202
7028	Type D	1.623489	2.86281	-0.6623	0.436852	0.000231	-0.10027	5.88716	2.9215E-06	4.0532		0.7521	0.7892
6422	Superpave C	1.627299	2.7724	-0.74671	0.478171	0.000394	-0.13115	7.25181	4.9238E-06	3.9100		0.7315	0.7234
7022	Superpave C	1.718919	2.71701	-0.77798	0.460811	0.000243	-0.10653	6.26777	5.2041E-06	3.8948		0.7423	0.7014
7622	Superpave C	1.812939	2.62804	-0.81532	0.461345	0.000221	-0.10051	5.95239	5.5095E-06	3.8792		0.7485	0.6756
6428	Superpave C	1.397739	3.05198	-0.69021	0.438707	0.000332	-0.11692	6.55884	2.6934E-06	4.0755		0.7315	0.7306
7028	Superpave C	1.604399	2.87056	-0.65845	0.439043	0.000232	-0.10044	5.8948	3.1804E-06	4.0299		0.7423	0.6986
6422	Superpave D	1.526169	2.90797	-0.8093	0.453715	0.000352	-0.12546	7.05795	4.0044E-06	3.9667		0.7465	0.8102
7022	Superpave D	1.744689	2.70832	-0.78465	0.458877	0.000242	-0.10639	6.26202	4.2081E-06	3.9531		0.7521	0.7792
7622	Superpave D	1.838989	2.61885	-0.82237	0.459783	0.00022	-0.10031	5.94372	4.4280E-06	3.9391		0.7609	0.7265
6428	Superpave D	1.423669	3.04585	-0.69351	0.435306	0.000326	-0.11604	6.52564	2.3989E-06	4.1073		0.7465	0.8202
7028	Superpave D	1.624919	2.86862	-0.66531	0.435749	0.000231	-0.10018	5.88316	2.8039E-06	4.0645		0.7521	0.7892
7622	SMA C	1.753092	2.64946	-0.81559	0.47702	0.000274	-0.10759	6.1878	9.2769E-08	4.9996		0.71	0.7761
7622	SMA D	1.743009	2.61438	-0.7972	0.479968	0.00028	-0.1085	6.22168	8.1315E-08	5.0358		0.7106	0.7856
7622	SMA F	1.746029	2.58684	-0.78233	0.482341	0.000285	-0.10921	6.24835	6.0576E-08	5.1166		0.7106	0.8004
7622	SMAR C	1.760879	2.64417	-0.79919	0.464972	0.000223	-0.10096	5.97228	9.2769E-08	4.9996		0.71	0.5406
7622	SMAR F	1.777739	2.57839	-0.7669	0.468496	0.000227	-0.10152	5.99597	6.0576E-08	5.1166		0.71	0.5514
7022	CAM	1.776609	2.51048	-0.5469	0.523773	-7.8E-05	-0.03639	2.93048	1.4129E-08	5.5159		0.767	1.354
7028	CMHB F	1.6275	2.8226	0.402	0.5965	0.000264	-0.08861	5.55391	1.0170E-08	4.0010		0.656	0.803

Note: SMAR stands for “stone-matrix asphalt rubber”; CMHB stands for “coarse matrix high binder”.

4.7 SUMMARY

This chapter discussed five types of key input parameters (dynamic modulus, cracking properties, rutting properties, FWD modulus, and LTE) from the TxACOL implementation point of view.

For each type of parameter, the laboratory or field determination method was illustrated to help users get in-depth knowledge and obtain accurate input parameters. Furthermore, the researchers developed some Excel macros and tools to ease the determination process. Finally, through assisting districts on overlay mix design and evaluation, the researchers proposed new default values for some mixtures, which will make engineers' design of asphalt overlays much easier.

CHAPTER 5.

TXACOL ENHANCEMENT

This chapter describes the TxACOL upgrading and calibration. Workshop feedback, default values, and findings from the field survey data analysis were all addressed or incorporated into the updated design system, and some new models were proposed and embedded into the software as well.

5.1 WORKSHOP FEEDBACK

Workshop attendees provided many useful comments regarding enhancement of the TxACOL. Comments included the following:

- Improve user input interface logic, such as removing/reorganizing some confusing input boxes.
- Allow for saving of project files automatically.
- Provide better prompting information for some input parameters.
- Optimize the output Excel files and graphs.
- Modify the analysis stop criteria, e.g., the analysis should stop according to design/analysis life rather than performance limit.
- Reduce running time.
- Incorporate more specific default values.
- Fix bugs.

Researchers addressed these comments, and the TxACOL is now more user friendly and convenient.

5.2 NEW RCR MODEL

As demonstrated in Chapter 3, 18 test sections were monitored and surveyed. The curves of RCR vs. months for most of the test sections were plotted. According to these curves, two important findings could be made:

- Many curves are much flatter than previous TxACOL-predicted curves.
- It is very common for RCR values to be larger than 50 percent.

The model used to determine RCR in the previous TxACOL is presented in Equation (5-1) (1).

$$RCR = \frac{100}{1 + e^{C_1 \log D}} \quad (5-1)$$

where

RCR = the reflective cracking rate (%).

C_1 = -4.2 is used based on previous research (1).

D = damage determined from Equation (5-2).

$$D = \sum \Delta C / h \quad (5-2)$$

where h is the overlay thickness and $\sum \Delta C$ is the total crack length.

Since $\sum \Delta C$ cannot be larger than h , the maximum D is 1; thus the maximum RCR is 50 percent according to Equation (5-1). The common curves of RCR vs. month predicted by the previous TxACOL are illustrated in Figure 5-1 (1).

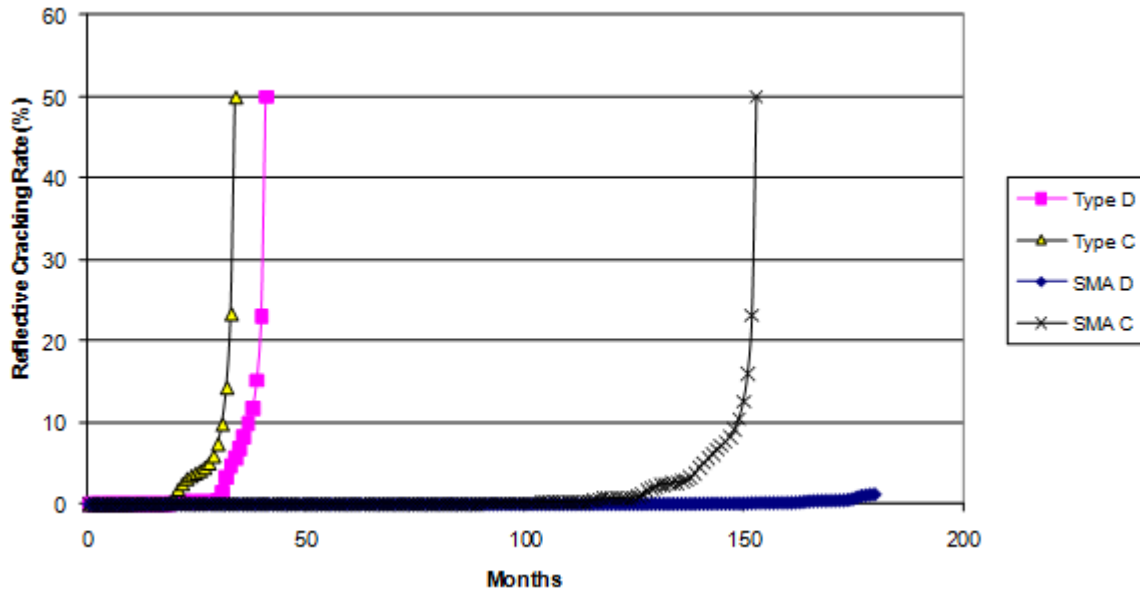


Figure 5-1. RCR Curves Determined by Previous TxACOL, after (1).

Figure 5-1 shows that the RCR curves are much steeper than the field survey result. To address this issue, the researchers proposed the following model:

$$RCR \% = 100 / \exp \left\{ \left[(\rho / m)^\beta \right] * constA \right\} \quad (5-3)$$

where

ρ = curve width.

β = curve slope.

m = month number.

$constA$ = 0.693147, which assures that when month number m equals curve width ρ , the RCR equals 50 percent.

This model derives from the s-shape empirical model employed in the National Cooperative Highway Research Program (NCHRP) Report 669 (7). The main differences between the proposed model and the model in NCHRP 669 are (a) the curve width ρ value can be directly determined based on the crack length incremental calculation; and (b) the adding of $constA$ assures that when total crack length $\sum \Delta C$ equals overlay thickness h , the RCR still equals 50 percent.

Figure 5-2 illustrates the curves following this ρ - β model. In this figure, three curves have the same ρ values (120 months) but different β values. This figure shows that these curves can be much flatter than previous TxACOL predictions and can predict the RCR values beyond 50 percent. It is believed that most of the previous surveyed curves can be better fitted by this model.

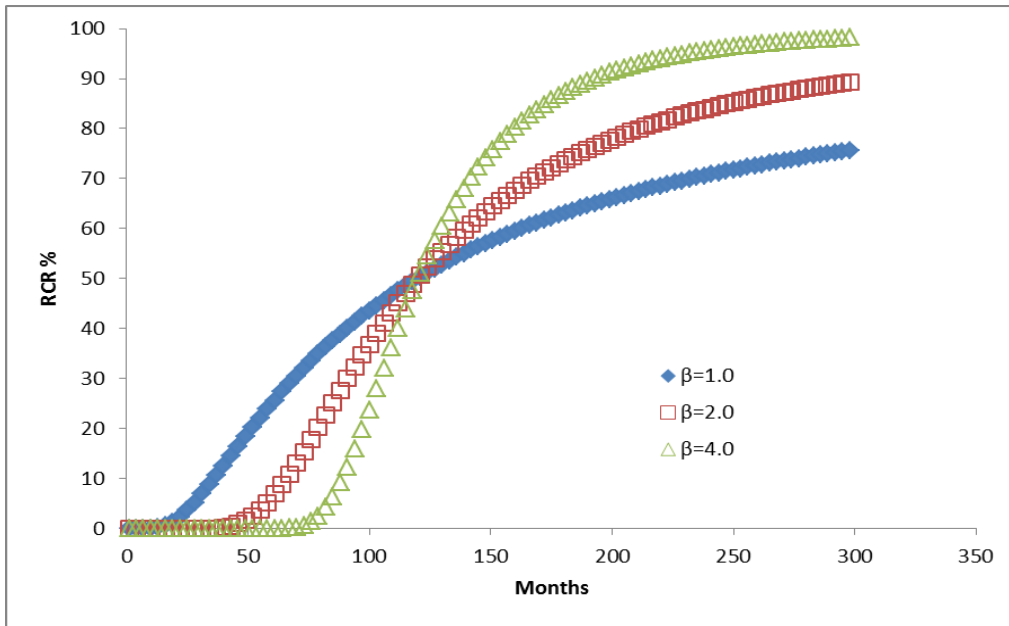


Figure 5-2. Curves of RCR Model ($\rho = 120$).

For incorporating the new model in the TxACOL, the ρ value (months) is directly determined based on the crack length incremental calculation—it equals the time (months) at the point when total crack length $\sum \Delta C$ equals overlay thickness h , while the slope β , the curve shape affecting parameter, is a calibration factor.

5.3 NEW THERMAL SIF MODEL ACCOUNTING FOR THE INFLUENCE OF THICK CTB LAYER

In Project 0-5123, the researchers employed a two-layer pavement structure (Asphalt overlay over existing Asphalt layer or PCC layer) to develop thermal SIF models (*I*). This structure implies an assumption that the layers under this two-layer structure are motionless under thermal variations and thus can be ignored. This assumption is appropriate for most cases since the thermal variation is not significant after a certain depth and the impact of base thermal movement can be ignored, especially for the granular base layer. However, as could be seen in some pavement structures, such as the SH 24 test section, the existing asphalt concrete (AC) layer was thin (3 inches), and the CTB layer on SH 24 was very thick (11 inches), over-cemented, and fully cracked (Figure 5-3), so the impact of thermal movement of this layer needed to be considered to make a more accurate prediction.

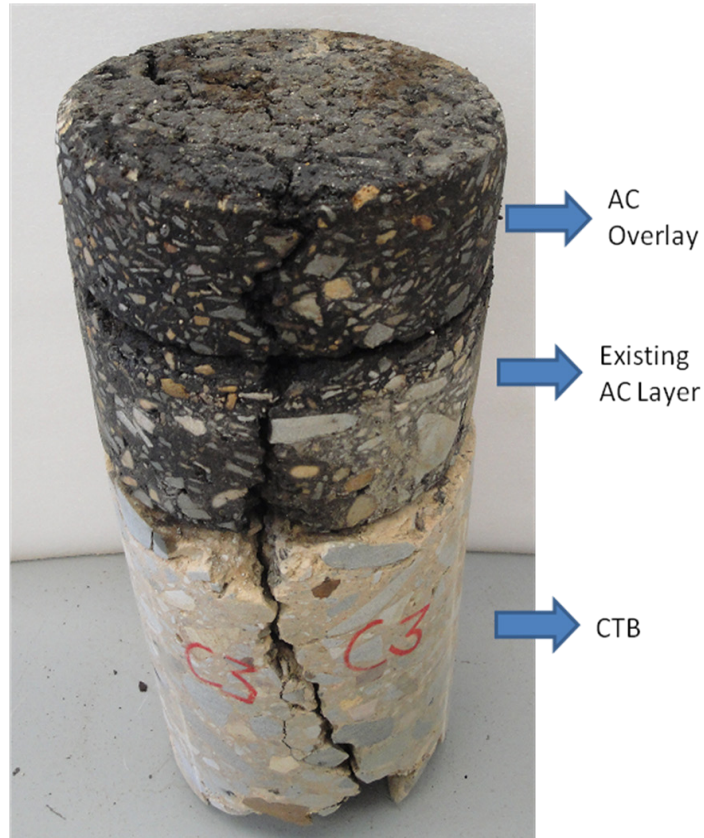


Figure 5-3. Cracked CTB Layer.

To address this issue, a three-layer AC/existing AC/CTB pavement structure, as shown in Figure 5-4, was considered, and the corresponding thermal SIF equations were developed.

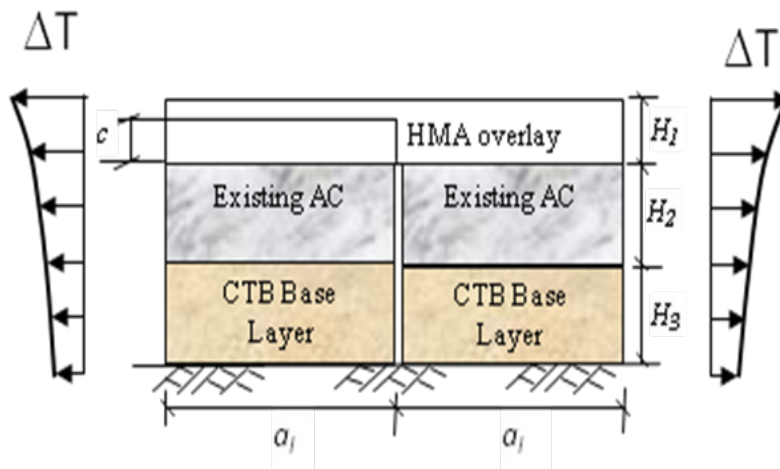


Figure 5-4. Three-Layer AC/Existing AC/CTB Pavement Structure Thermal SIF Model.

To develop a representative SIF equation, different combinations, such as different layer thickness, layer modulus, and coefficients of thermal expansion (CTEs), were included, and 58,320 SIFs were calculated using a specifically developed finite element program (8).

Employing Microsoft Excel Solver, the final SIF equations were developed and are presented below:

$$K_{thermal} = K_a \times \left[K_b \left(\frac{c}{H_1} \right)^3 + K_c \left(\frac{c}{H_1} \right)^2 + K_d \left(\frac{c}{H_1} \right) + K_e \right] \times \sigma_{far} \quad (5-4)$$

$$K_a = 0.6131 - 0.9984c^{-0.3416} + 0.1251 \log H_1 - 0.2311 \log H_2 + 2.1198 \times \left(\frac{\alpha_1}{\alpha_2} \right)^{-1.2211} \\ + 0.0205 \log a_l - 0.0085 \times \left(\frac{\alpha_2}{\alpha_3} \right)^{1.8677} - 0.0037 \log H_3 + 0.1117 \log E_3 \quad (5-5)$$

$$K_b = 131.472 - 0.4622c^{0.2516} - 19.5848 \log H_1 - 2.8503 \log H_2 - 3.5861 \times \left(\frac{\alpha_1}{\alpha_2} \right)^{-0.3596} \\ + 1.7685 \log a_l - 3.446 \times 10^{-5} \times \left(\frac{\alpha_2}{\alpha_3} \right)^{-30.0457} - 8.4905 \log H_3 - 5.0097 \log E_3 \quad (5-6)$$

$$K_c = -419.939 + 100.9409c^{-0.1776} + 41.5705 \log H_1 + 7.5717 \log H_2 + 5.4687 \times \left(\frac{\alpha_1}{\alpha_2} \right)^{0.8264} \\ + 2.6716 \log a_l + 159.084 \times \left(\frac{\alpha_2}{\alpha_3} \right)^{-0.0014} + 12.883 \log H_3 + 6.1387 \log E_3 \quad (5-7)$$

$$K_d = 95.365 - 19.4183c^{-1.4503} - 11.7225 \log H_1 - 4.0916 \log H_2 - 0.0049 \times \left(\frac{\alpha_1}{\alpha_2} \right)^{6.6874} \\ - 1.1782 \log a_l - 6.073 \times \left(\frac{\alpha_2}{\alpha_3} \right)^{-0.1088} - 5.4581 \log H_3 - 3.2133 \log E_3 \quad (5-8)$$

$$K_e = -36.5495 + 25.383c^{-0.2223} + 5.123 \log H_1 + 1.024 \log H_2 + 5.063 \times \left(\frac{\alpha_1}{\alpha_2} \right)^{0.4903} \\ + 0.1764 \log a_l + 2.4119 \times \left(\frac{\alpha_2}{\alpha_3} \right)^{-1.0224} + 0.4095 \log H_3 + 1.2911 \log E_3 \quad (5-9)$$

where

c = crack length in the overlay.

H_1 = overlay thickness.

H_2 = existing AC layer thickness.

H_3 = base layer thickness.

α_1 , α_2 , and α_3 = CTEs of overlay, existing AC layer, and base layer, respectively.

E_3 = modulus of base layer.

a_l = half crack spacing.

σ_{far} = thermal stress at the point that is at the middle of the cracking space and at the same height as the crack tip.

All these new SIF equations for AC/existing AC/CTB were incorporated into the TxACOL. In terms of user interface, when users select “Stabilized Base,” one more input box will show up that lets users input the CTE for the base layer. See Figure 5-5.

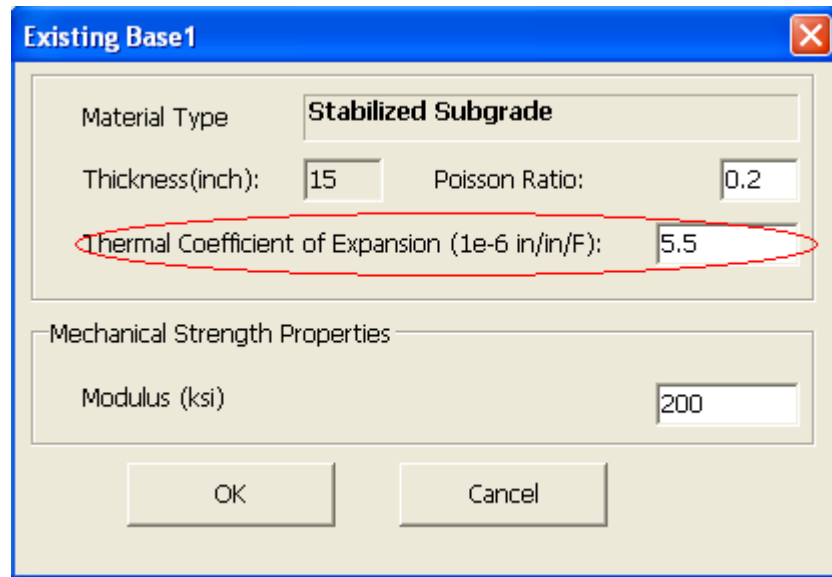


Figure 5-5. CTE Input for CTB Layer.

5.4 LTE STANDARD DEVIATION CONSIDERATION

As mentioned in Chapter 4, not only the LTE mean value but also the standard deviation of LTE is required as input in the TxACOL. To consider the influence of the LTE standard deviation (LTE STD), the following algorithm was proposed for RCR determination.

- Step 1: Determine the monthly RCR values based on LTE (%) mean value and new RCR model (ρ - β model).
- Step 2: Determine the monthly RCR values based on LTE (%) mean + LTE STD value and ρ - β model.
- Step 3: Determine the monthly RCR values based on LTE (%) mean – LTE STD value and ρ - β model.
- Step 4: Average the monthly RCR values determined from Step 1 to Step 3.

Figure 5-6 illustrates the formation of RCR vs. month curve for LTE (%) mean value 70 with standard deviation 10. Three RCR curves according to LTE (%) 60, 70, and 80 were determined and then averaged to the result curve.

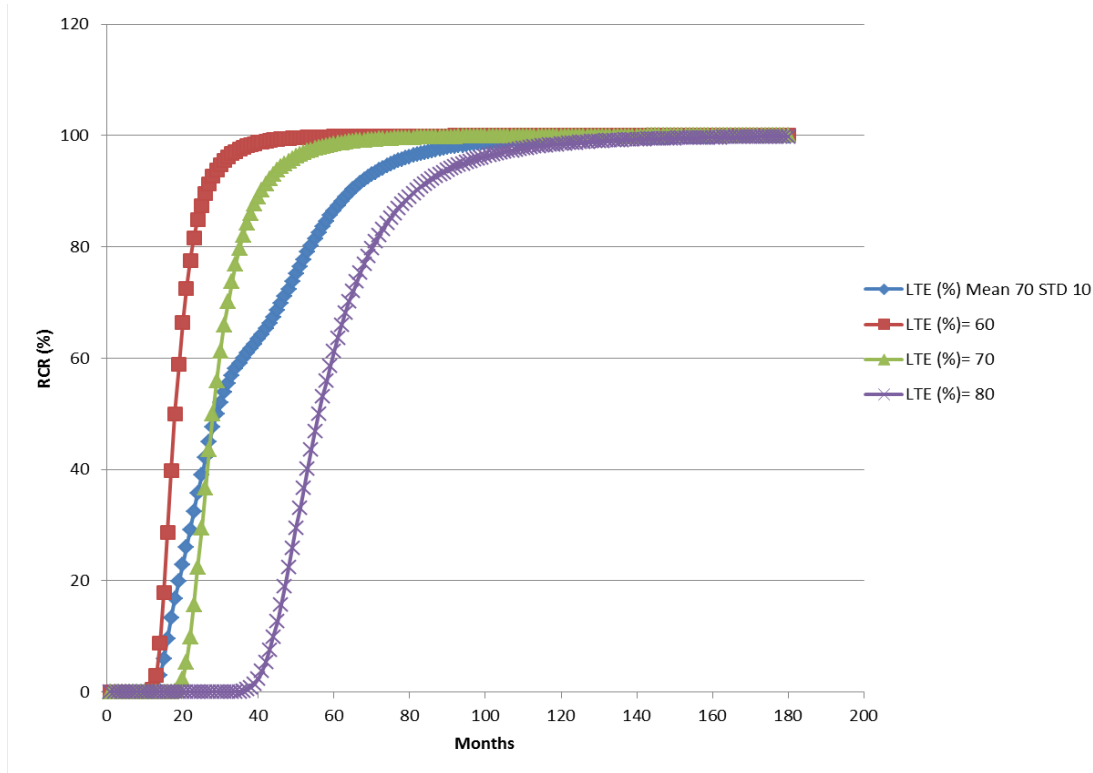


Figure 5-6. RCR Curves Accounting for LTE STD.

5.5 CALIBRATION FACTORS

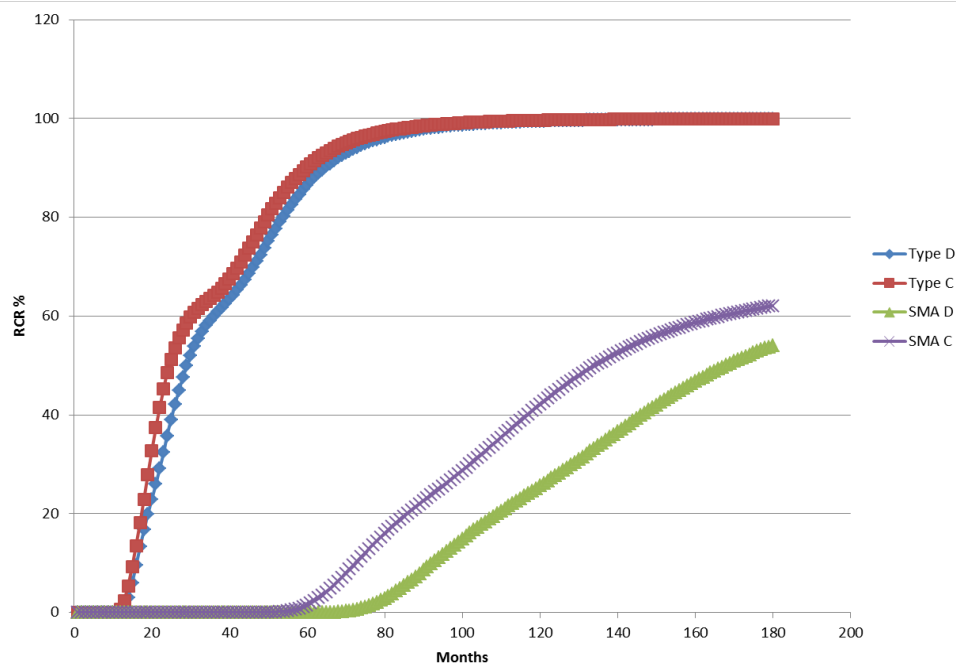
Since the RCR models, default value database, and SIF models were updated in the TxACOL, the relevant sensitivity analyses were conducted, and the calibration factors were fine-tuned.

Figures 5-7 to 5-10 illustrate the RCR predictions influenced by overlay mix type, thickness, traffic, and LTE STD, respectively.

Figure 5-7 shows the influence of AC type. The other main input parameters are the following:

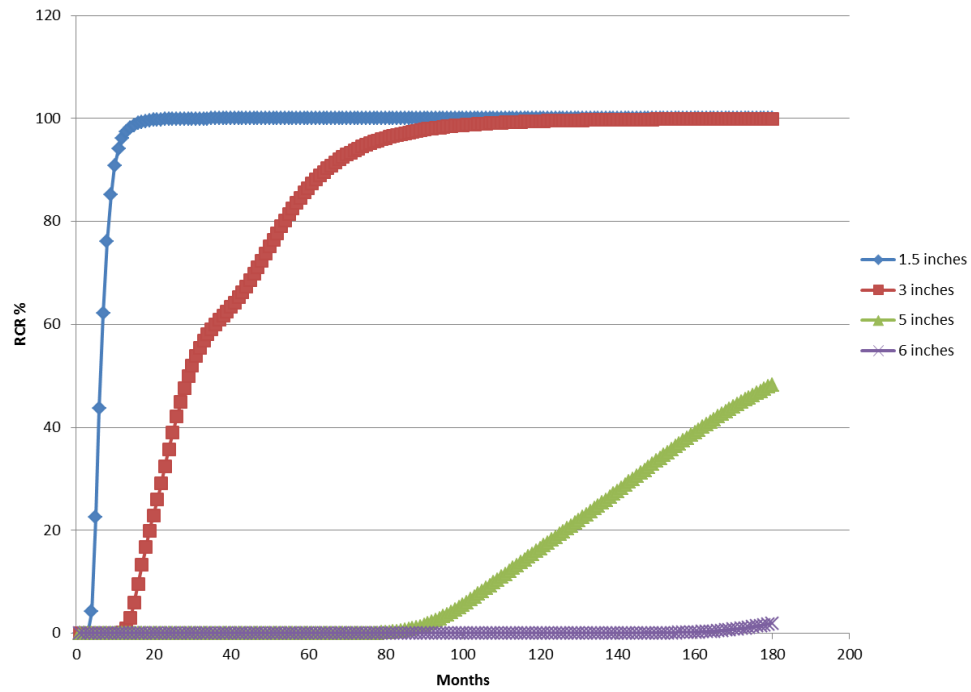
- Pavement structure type: AC over Jointed Plain Concrete Pavement (JPCP).
- AC overlay thickness: 3 inches.
- Binder type: PG 76-22.
- JPCP Modulus: 4000 ksi.

- JPCP thickness: 10 inches.
- JPCP LTE% mean: 70; STD: 10.
- Subgrade modulus: 8 ksi.
- Climate weather station: Austin.
- Traffic (equivalent single axle loads [ESALs] of 20 years, millions): 10.



Figures 5-7. Influence of Overlay Mix Type.

Figure 5-8 shows the influence of overlay thickness. The other main input parameters are the same as in Figure 5-7, except the AC type is fixed to Type D.



Figures 5-8. Influence of Overlay Thickness.

Figure 5-9 shows the influence of traffic. The other main input parameters are the same as in Figure 5-7, except the AC type is fixed to Type D.

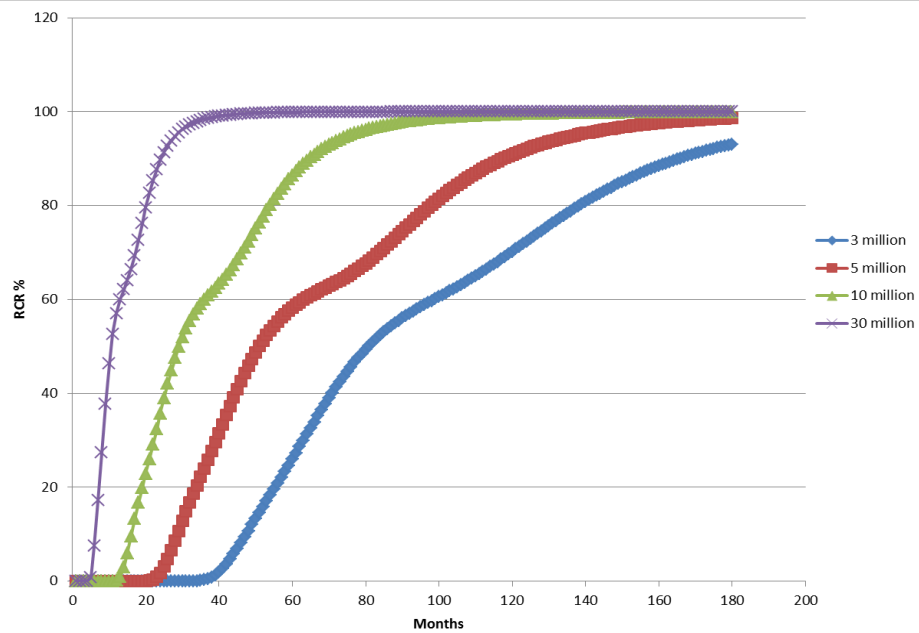


Figure 5-9. Influence of Traffic.

Figure 5-10 shows the influence of LTE STD. The other main input parameters are the same as in Figure 5-7, except the AC type is fixed to Type D. In this figure, all RCR curves of different LTE STD arrive at 50 at the same month since they have the same LTE mean value. Larger LTE STD will lead to higher monthly RCR (%) values before arriving at 50 and lower RCR values after passing 50. This makes sense because the larger LTE STD means more scattered crack performance.

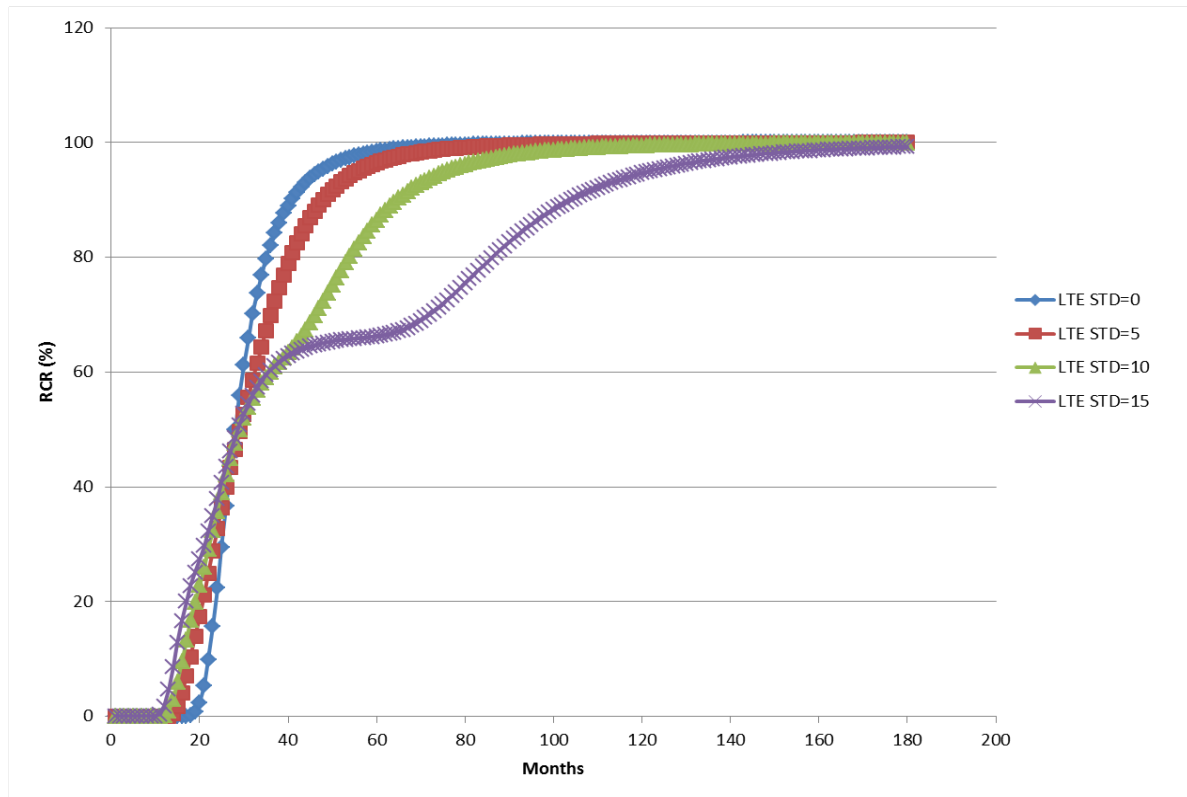


Figure 5-10. Influence of LTE STD.

According to numerous pilot calculations and sensitivity analyses, currently, the calibration factors k_1 (for bending) and k_2 (for shearing) are refined to 15 and 30, respectively (previously, they were 20 and 40). The default value of β is proposed to be 5.0 in the TxACOL for now. It might need further refining according to a different LTE standard deviation, since the larger the LTE standard deviation, the flatter the RCR curve will be. Correspondingly, the β might be smaller. More real cases will help to further refine these calibration factors.

5.6 SUMMARY

This chapter discussed how researchers used workshop comments, field survey data analysis findings, new models/algorithms, sensitivity analyses, and calibration factors to enhance the TxACOL. More specifically, researchers:

- Briefly introduced the update of the TxACOL based on workshop comments.
- Proposed a ρ - β model to be incorporated into the TxACOL. Researchers found that this model could fit most of the surveyed RCR curves. The ρ value, which represents the curve width, can be determined directly based on the crack length incremental calculation, while the β value (curve slope) can be the calibration factor.
- Discussed the new thermal SIF model considering the influence of a thick CTB layer that was developed and incorporated into the TxACOL.
- Proposed a specific algorithm to account for LTE STD during RCR calculation.
- Described the numerous pilot calculations and sensitivity analyses that were conducted and the calibration factors that were refined. More data from other candidate test sections will help with further refinement of these factors.

CHAPTER 6. CASE STUDIES

This chapter demonstrates the comparisons between the TxACOL RCR predictions and field survey results for four test sections: three test sections on IH 40 and one test section on SH 24.

6.1 CASE 1: IH 40 TEST SECTIONS

As stated in Chapter 3, four test sections on IH 40 were surveyed. Among them, three overlay test sections (section 1, section 2, and section 3) were identified as candidates for TxACOL prediction. Section 0 was excluded because no existing pavement evaluation was conducted before construction.

For the three identified test sections, each existing crack was recorded and photographed before the overlay construction on August 11, 2009. An FWD test was run on the milled surface through these test sections. Plant mixes for each test section were sampled at the construction site as well. Thus, these test sections were good candidates for case study. Figure 6-1 presents the existing pavement conditions.



Figure 6-1. Existing Pavement Condition of IH 40 Test Sections.

Figure 6-2 shows an example (test section 2) of how the cracks were recorded in the Excel file. Note in this figure, the survey on 8/11/2009 was conducted just before the overlay construction, thus 42 was the total existing number of cracks. The RCR value can be calculated as the ratio of reflected cracking number over existing cracking number. For example, 12 was the reflected cracking number on April 5, 2011, the RCR value could then be determined as 12/42, which equals 28.6 percent.

		42		0		12		16		24	
Cracking Number	Distance from beginning (ft)	8/11/2009		9/8/2010		4/5/2011		12/15/2011		5/30/2012	
start (No crack)	2608	3008	view	2408	view	3297	view	943	view	3744	view
68	2628	3009	view							3746	view
69	2663	3010	view							3747	view
70	2685	3011	view			3298	view	946	view	3748	view
71	2707	3012	view							3749	view
72	2730	3013	view			3299	view	947	view	3750	view
73	2751	3014	view							3751	view
74	2773	3015	view							3752	view
75	2790	3016	view							3753	view
76	2807	3017	view			3300	view	948	view	3754	view
77	2826	3018	view							3755	view
78	2854	3019	view			3301	view	949	view	3756	view
79	2867	3020	view							3757	view
80	2894	3021	view							3758	view

Figure 6-2. Crack Survey Recording Excel File for IH 40 Test Section.

The corresponding surveyed RCR values of each test section were tabulated and plotted in Chapter 3 (Table 3-8 and Figure 3-25, respectively).

To predict RCR and compare with the survey results, some key input parameters to the TxACOL have to be determined first. As discussed in Chapter 4, these key input parameters for RCR prediction are: FWD modulus, LTE, dynamic modulus, and cracking property. The following sections demonstrate the parameters determination process and present parameter values as well.

6.1.1 FWD Modulus Back-Calculation

Figure 6-3 shows the FWD test on the milled surface before the overlay construction on IH 40. The FWD modulus back-calculation method was discussed in Chapter 4. For these three test sections on IH 40, the FWD loads were applied not only on the slab center (for AC pavement,

the slab center means the middle position between two cracks), but also at the edge of the slab (at one side of the joint/crack).



Figure 6-3. FWD Test on IH 40 Test Sections.

As discussed in Chapter 4, *Modulus 6.0* was employed to back-calculate the pavement structure modulus. The main input parameters, such as pavement structure thickness and modulus range, are presented in Figure 6-4. The pavement structure information can be found in Figure 3-22 in Chapter 3.

The 'Modulus Input' dialog box contains the following fields and controls:

- Distance to plate:** Seven input boxes with values 0.0, 12.0, 24.0, 36.0, 48.0, 60.0, and 72.0.
- Layer:** Radio buttons for 'Two', 'Three' (selected), and 'Four'.
- Semi-Infinite:** A checked checkbox.
- Thickness (in):** Three rows:
 - Surface: 10.00, Asphalt Temp. 75.0
 - Base: 12.00, Other Material (dropdown)
 - Subgrade: Other Material (dropdown)
- MODULI RANGE (ksi):**
 - Minimum: 340.0, Maximum: 1040.0, Poisson's Ratio: 0.38
 - 50.0, 300.0, 0.30
 - Most Probable Value: 15.0, 0.35
- Set as default value:** A checked checkbox.
- Buttons:** 'Exit' and 'Run'.

Figure 6-4. Input Parameters for Modulus Back-Calculation.

Because the FWD data file contains the deflection basin data on cracks/joints, to enhance the accuracy, the station points were re-selected, and all the deflection basin data on cracks/joints were unchecked and thus not involved in back-calculation. See Figure 6-5.

	No	STATION	LOAD	W1	W2	W3	W4	W5	W6	W7	PVMT	AIR	SURF	TIME	DTB	Comment	
<input type="checkbox"/>	1	0	12227	18.2	11.8	7.7	5.1	3.7	2.9	2.3	0	77	0	10:39	224		<input type="checkbox"/>
<input checked="" type="checkbox"/>	2	13	11457	8.9	8.0	6.3	4.6	3.5	2.9	2.2	0	77	0	10:39	300 *		<input checked="" type="checkbox"/>
<input type="checkbox"/>	3	26	11508	17.1	9.4	7.1	4.5	3.4	3.0	2.2	0	76	0	10:41	185 *		<input type="checkbox"/>
<input checked="" type="checkbox"/>	4	38	11874	9.1	8.3	6.4	4.7	3.7	3.0	2.3	0	76	0	10:42	136		<input checked="" type="checkbox"/>
<input type="checkbox"/>	5	47	11258	15.4	7.1	5.8	4.2	3.3	2.9	2.3	0	76	0	10:42	300 *		<input type="checkbox"/>
<input checked="" type="checkbox"/>	6	66	11787	8.5	7.7	6.0	4.4	3.3	2.7	2.1	0	76	0	10:43	158		<input checked="" type="checkbox"/>
<input type="checkbox"/>	7	82	11214	17.8	10.5	5.7	4.1	3.1	2.6	2.1	0	76	0	10:44	249 *		<input type="checkbox"/>
<input checked="" type="checkbox"/>	8	103	11600	9.8	8.0	6.2	4.5	3.4	2.8	2.1	0	76	0	10:44	300		<input checked="" type="checkbox"/>
<input type="checkbox"/>	9	123	11151	20.9	10.0	6.9	4.6	3.4	2.9	2.2	0	76	0	10:45	300 *		<input type="checkbox"/>
<input checked="" type="checkbox"/>	10	134	11628	9.7	8.5	6.7	4.9	3.7	3.1	2.4	0	76	0	10:46	300		<input checked="" type="checkbox"/>
<input checked="" type="checkbox"/>	11	144	10972	13.6	12.3	6.6	4.7	3.7	3.0	2.4	0	76	0	10:47	300 *		<input checked="" type="checkbox"/>
<input checked="" type="checkbox"/>	12	155	12025	8.4	7.9	6.5	5.0	3.9	3.2	2.4	0	76	0	10:48	131		<input checked="" type="checkbox"/>
<input type="checkbox"/>	13	167	11012	23.4	9.1	6.8	5.0	3.8	3.2	2.5	0	76	0	10:48	300 *		<input type="checkbox"/>
<input checked="" type="checkbox"/>	14	183	12045	10.1	8.9	7.3	5.3	4.1	3.2	2.5	0	76	0	10:49	148		<input checked="" type="checkbox"/>
<input type="checkbox"/>	15	198	11361	24.9	14.7	8.9	5.6	4.0	3.3	2.6	0	76	0	10:50	186 *		<input type="checkbox"/>

Figure 6-5. Station Selection for Modulus Back-Calculation.

Figure 6-6 presents the final modulus back-calculation result. The existing AC modulus, 530.8 ksi, and the base modulus, 53 ksi, were used as input for the TxACOL prediction.

TTI MODULUS ANALYSIS SYSTEM (SUMMARY REPORT)														(Version 6.0)	
District:									MODULI RANGE (psi)						
County :									Minimum				Poisson Ratio Values		
Highway/Road:									Maximum				H1: v = 0.38		
									Base: 12.00 50,000 300,000				H2: v = 0.30		
									Subbase: 0.00				H3: v = 0.00		
									Subgrade: Semi-Infinite 15,000				H4: v = 0.35		
Station	Load (lbs)	Measured Deflection (mils):							Calculated Moduli values (ksi):				Absolute Dpth to		
		R1	R2	R3	R4	R5	R6	R7	SURF (E1)	BASE (E2)	SUBB (E3)	SUBG (E4)	ERR/Sens Bedrock		
13.000	11,456	8.89	7.97	6.29	4.59	3.49	2.93	2.19	759.8	55.6	0.0	18.5	5.04 300.0 *		
38.000	11,873	9.05	8.25	6.41	4.66	3.65	3.04	2.28	792.8	56.3	0.0	18.6	5.02 135.7 *		
66.000	11,786	8.53	7.68	6.02	4.37	3.34	2.71	2.10	784.3	60.3	0.0	20.1	5.51 158.1 *		
103.000	11,599	9.83	8.03	6.19	4.45	3.37	2.77	2.14	529.4	58.6	0.0	19.5	4.25 300.0 *		
134.000	11,627	9.73	8.53	6.71	4.88	3.72	3.07	2.43	661.1	53.3	0.0	17.8	4.87 300.0 *		
144.000	10,971	13.57	12.25	6.60	4.72	3.67	3.04	2.38	340.0	50.0	0.0	15.7	12.74 300.0 *		
155.000	12,024	8.41	7.91	6.45	4.97	3.87	3.15	2.37	1040.0	59.8	0.0	17.9	4.68 131.3 *		
183.000	12,044	10.06	8.93	7.26	5.25	4.07	3.24	2.45	723.5	51.3	0.0	17.1	5.17 147.9 *		
208.000	11,925	9.76	8.76	6.99	5.15	3.91	3.25	2.46	746.9	51.4	0.0	17.1	4.93 300.0 *		
218.000	11,507	18.43	20.40	6.95	5.03	3.83	3.16	2.51	340.0	50.0	0.0	13.9	28.51 31.9 *		
228.000	12,203	10.18	9.28	7.16	5.17	3.88	3.16	2.39	645.5	53.0	0.0	17.7	6.23 300.0 *		
239.000	12,111	9.97	8.71	6.77	4.68	3.85	3.15	2.43	644.5	55.2	0.0	18.4	4.84 300.0 *		
278.000	11,555	9.86	8.63	6.62	4.77	3.58	2.95	2.28	580.7	54.4	0.0	18.1	5.46 300.0 *		
301.000	11,591	12.66	13.31	5.62	4.23	3.26	2.76	2.18	340.0	55.4	0.0	18.5	15.75 63.5 *		
314.000	11,388	9.50	7.68	6.00	4.36	3.37	2.69	2.07	561.5	58.8	0.0	19.6	3.59 153.2 *		
348.000	12,012	9.16	8.04	6.29	4.70	3.67	2.93	2.32	772.2	57.3	0.0	19.1	4.08 177.8 *		
2032.000	11,384	10.56	8.57	6.37	4.52	3.43	2.86	2.20	434.7	56.3	0.0	18.8	4.62 300.0 *		
2086.000	12,048	7.62	6.70	5.31	3.90	3.05	2.50	1.92	952.7	68.4	0.0	22.8	4.28 142.4 *		
2109.000	11,646	15.24	13.73	6.00	4.35	3.27	2.62	2.14	340.0	50.0	0.0	16.7	24.26 77.7 *		
2129.000	11,639	8.75	7.60	5.94	4.28	3.22	2.54	1.97	662.2	61.7	0.0	20.6	5.67 160.0 *		
2169.000	11,623	10.33	9.01	6.81	4.80	3.56	2.83	2.17	497.9	54.7	0.0	18.2	6.79 299.3 *		
2287.000	11,833	9.61	8.31	6.40	4.54	3.38	2.73	2.14	574.3	58.7	0.0	19.6	6.09 300.0 *		
2351.000	11,778	9.09	7.95	6.13	4.42	3.34	2.75	2.15	656.2	59.7	0.0	19.9	5.29 300.0 *		
2480.000	12,242	8.64	7.57	5.92	4.35	3.34	2.80	2.22	808.7	62.7	0.0	20.9	4.32 300.0 *		
2525.000	11,420	12.06	9.63	7.03	4.93	3.67	3.04	2.36	381.1	50.0	0.0	16.7	6.70 300.0 *		
2562.000	11,364	10.31	9.13	7.20	5.22	3.98	3.21	2.52	603.9	50.0	0.0	16.3	5.42 186.3 *		
2617.000	11,055	11.34	9.36	7.20	5.11	3.73	3.02	2.30	406.3	50.0	0.0	16.5	5.81 254.6 *		
2637.000	11,106	22.29	19.46	7.13	4.86	3.64	2.99	2.39	340.0	50.0	0.0	13.2	33.53 38.8 *		
2665.000	11,766	11.99	10.29	7.62	5.11	3.62	2.86	2.19	397.9	50.0	0.0	16.7	10.93 192.3 *		
2716.000	11,353	10.29	8.90	6.87	4.89	3.62	2.93	2.25	516.3	52.5	0.0	17.5	6.06 295.4 *		
2746.000	11,686	13.87	14.48	6.02	4.49	3.46	2.83	2.27	340.0	52.0	0.0	17.3	17.93 59.5 *		
2775.000	11,492	10.25	8.67	6.63	4.67	3.46	2.77	2.15	483.0	55.8	0.0	18.6	6.20 294.5 *		
2815.000	12,211	9.39	8.39	6.53	4.66	3.46	2.80	2.19	659.9	59.2	0.0	19.7	6.42 286.6 *		
2870.000	11,869	9.90	8.15	6.29	4.50	3.41	2.84	2.21	546.4	59.0	0.0	19.7	4.35 300.0 *		
Mean:		12.89	10.30	6.96	4.95	3.75	3.06	2.38	530.8	53.0	0.0	16.9	10.11 219.6		
Std. Dev:		4.38	2.95	0.79	0.43	0.30	0.24	0.19	195.0	8.8	0.0	2.2	7.72 186.6		
Var Coeff(%):		33.98	28.65	11.31	8.73	7.97	7.82	7.97	36.7	7.3	0.0	13.1	76.38 85.0		

Figure 6-6. Modulus Back-Calculation Result.

6.1.2 LTE Determination

Researchers used the same FWD data used in the modulus back-calculation for the LTE determination. Following the method illustrated in Chapter 4, the LTE values for each crack in the test sections were calculated. Some calculated LTE values were larger than 100 and were excluded. The final result is summarized in Table 6-1.

Table 6-1. LTE Values for IH 40 Test Sections.

Test Section	Mean LTE (%)	LTE STD
1	65.9	19.4
2	81.5	11.6
3	73.3	14.8

6.1.3 Material Property of Asphalt Overlay Mix

The overlay material of each test section was as follows: Section 1—0% RAP, PG 64-28, designed by the contractor; section 2—35% RAP, AC-10, designed by TTI; and section 3—20% RAP, PG 64-28, designed by TTI. The plant mixes for each test section were collected during

construction, and the dynamic modulus samples and OT samples were molded in the lab and tested.

Tables 6-2 to 6-4 present the dynamic modulus results for each test section.

Table 6-2. Dynamic Modulus (ksi) for IH 40 Test Section 1 (0% RAP, PG 64-28).

Temperature(°F)	Frequency (Hz)					
	25	10	5	1	0.5	0.1
14	2275	2163	1985	1597	1433	1090
40	1775	1555	1367	1012	856	587
70	817	612	481	263	195	110
100	228	145	101	46	36	24
130	103	61	40	21	16	12

Table 6-3. Dynamic Modulus (ksi) for IH 40 Test Section 2 (35% RAP, AC-10).

Temperature(°F)	Frequency (Hz)					
	25	10	5	1	0.5	0.1
14	3746	3566	3370	2953	2758	2283
40	2550	2322	2119	1705	1545	1159
70	1190	953	779	457	364	197
100	341	213	152	65	50	29
130	116	68	46	22	16	12

Table 6-4. Dynamic Modulus (ksi) for IH 40 Test Section 3 (20% RAP, PG 64-28).

Temperature(°F)	Frequency (Hz)					
	25	10	5	1	0.5	0.1
14	3171	2913	2681	2231	2036	1571
40	2164	1914	1719	1299	1146	803
70	998	739	615	353	273	149
100	281	177	123	54	41	25
130	204	143	99	54	41	30

For each test section, five OT samples were molded to determine fracture property A and n values. The new tool (demonstrated in Chapter 4) for handling multiple OT data files and determining the A and n values based on average load reduction curve was employed. The A and

n values for each test section are listed in Table 6-5. These values will be used as input for TxACOL prediction as well.

Table 6-5. A and n Values for IH 40 Test Sections.

	A	n
Amarillo—IH 40 Test Section 1 Plant Mix (0% RAP, PG 64-28)	4.9318E-07	4.5009
Amarillo—IH 40 Test Section 2 Plant Mix (35% RAP, AC-10)	1.1495E-06	4.2061
Amarillo—IH 40 Test Section 3 Plant Mix (20% RAP, PG 64-28)	4.9975E-07	4.3948

6.1.4 TxACOL Prediction for IH 40 Test Sections

Per previous discussion, the following input parameters were collected:

- FWD back-calculated modulus for existing AC and base.
- LTE values for each test section.
- Dynamic modulus of overlay mixture for each test section.
- Fracture properties A and n of overlay mixture for each test section.
- Pavement structure (4 inches of overlay, 10 inches of existing AC, 12 inches of base, and subgrade).
- Climatic data from Amarillo weather station.

After incorporating all these parameters into the TxACOL, the RCR prediction for each test section was made and compared with the surveyed RCR curves. See Figures 6-7, 6-8, and 6-9.

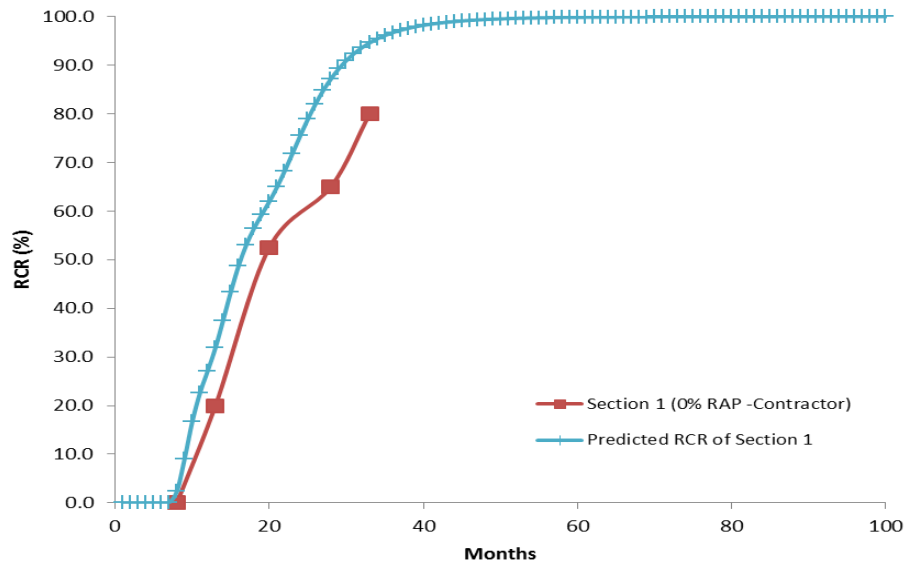


Figure 6-7. RCR Prediction and Survey Result of IH 40 Test Section 1.

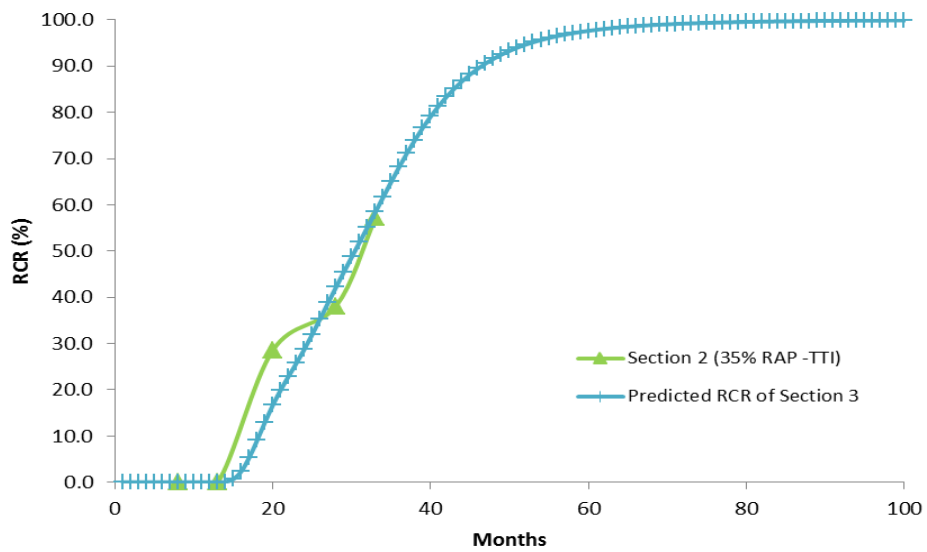


Figure 6-8. RCR Prediction and Survey Result of IH 40 Test Section 2.

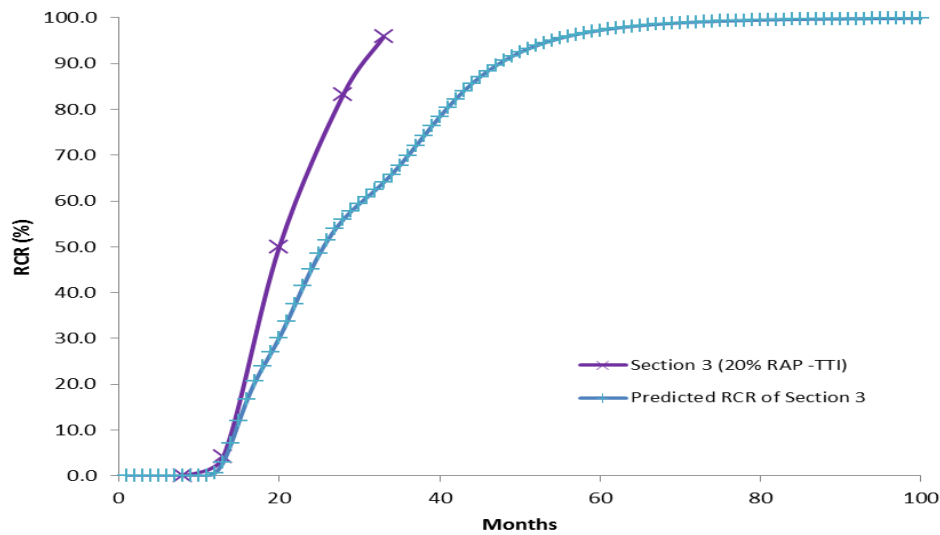


Figure 6-9. RCR Prediction and Survey Result of IH 40 Test Section 3.

6.2 CASE 2: SH 24 TEST SECTION

A 4000 ft test section was selected on SH 24. The overlay pavement structure consisted of 2.5 inches of Type D mix, 3 inches of Type B asphalt concrete, 11 inches of cement-treated base, 8 inches of lime treated subgrade, and natural subgrade.

The 2.5 inches of asphalt overlay was constructed in July 2009. Existing cracks before the asphalt overlay were numbered, photographed, and mapped. A total of 61 transverse cracks with different severities were identified in the selected test section. Figure 6-10 presents the detailed cracking map surveyed on July 2, 2009. The original design of asphalt overlay mix used on SH 24 is presented in Figure 6-11.

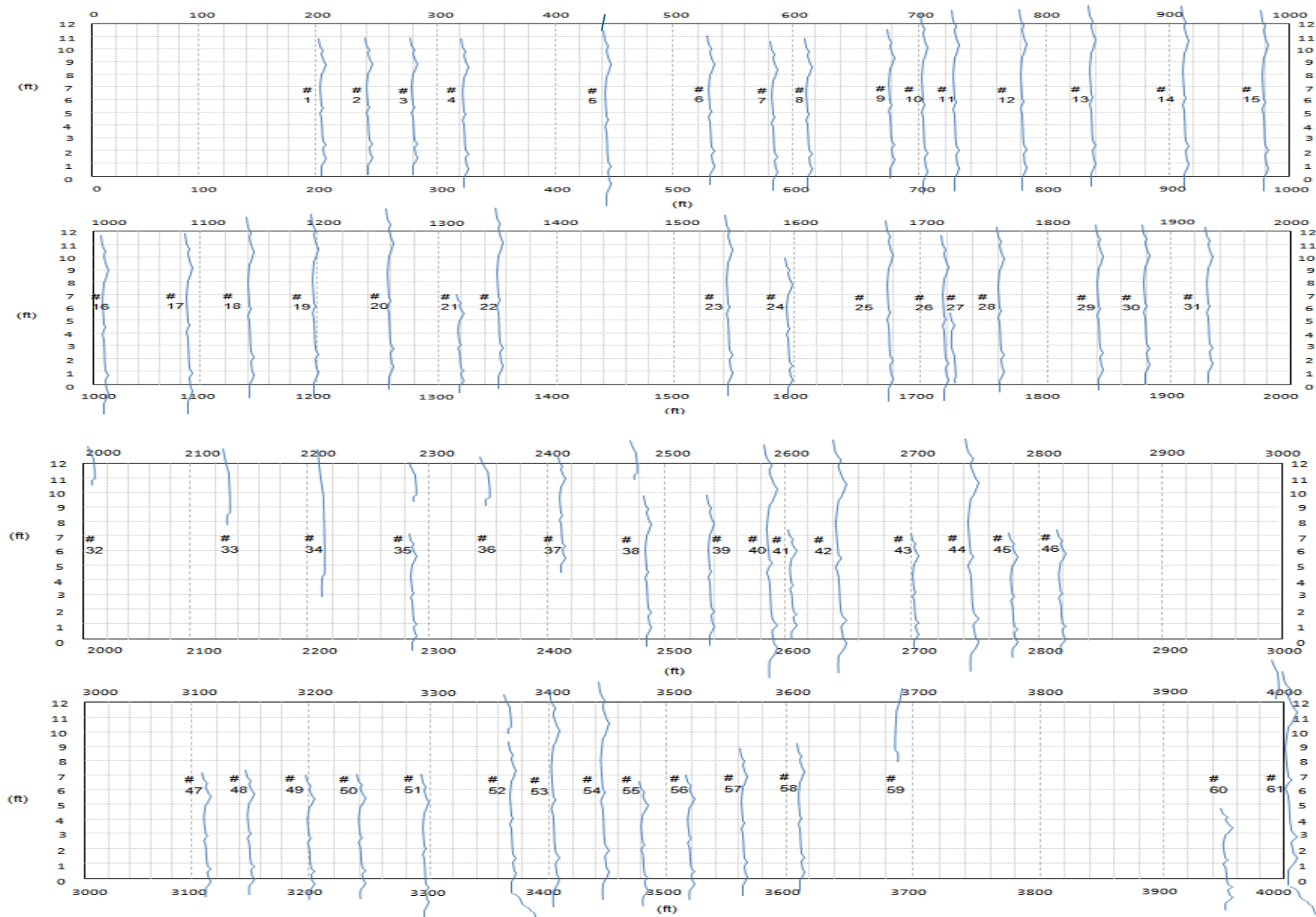


Figure 6-10. Cracking Map of SH 24 Test Section before Asphalt Overlay Construction.

BIN FRACTIONS																									
	Bin No.1	Bin No.2	Bin No.3	Bin No.4	Bin No.5	Bin No.6	Bin No.7																		
Aggregate Source:	MARTIN MARIETTA	MARTIN MARIETTA	Drake																						
Aggregate Pit:	SAWYER, OK	SAWYER, OK																							
Aggregate Number:																									
Sample ID:	D ROCK	SCREENINGS	River Sand																						
Rap?:																									
							Total Bin																		
Individual Bin (%):	60.0	Percent	30.0	Percent	10.0	Percent	0.0	Percent	0.0	Percent	0.0	Percent	0.0	Percent	100.0%	Lower & Upper Specification Limits			Restricted Zone			Individual % Retained	Cumulative % Retained	Sieve Size	
Sieve Size:	Cum.% Passing	Wtd Cum. %	Cum.% Passing	Wtd Cum. %	Cum.% Passing	Wtd Cum. %	Cum.% Passing	Wtd Cum. %	Cum.% Passing	Wtd Cum. %	Cum.% Passing	Wtd Cum. %	Cum.% Passing	Wtd Cum. %	Cum. % Passing	Lower	Upper	Within Spec's	Lower	Upper	Within Spec's				
3/4"	100.0	60.0	100.0	30.0	100.0	10.0			100.0	0.0	100.0	0.0	100.0	0.0	100.0	100.0	100.0	Yes				0.0	0.0	3/4"	
1/2"	100.0	60.0	100.0	30.0	100.0	10.0			100.0	0.0	100.0	0.0	100.0	0.0	100.0	98.0	100.0	Yes				0.0	0.0	1/2"	
3/8"	95.3	57.2	100.0	30.0	99.3	9.9			95.3	0.0	100.0	0.0	100.0	0.0	97.1	85.0	100.0	Yes				2.9	2.9	3/8"	
No. 4	34.5	20.7	98.9	29.7	99.0	9.9			34.5	0.0	98.9	0.0	91.3	0.0	60.3	50.0	70.0	Yes				36.8	39.7	No. 4	
No. 8	12.0	7.2	77.6	23.3	98.3	9.8			12.0	0.0	77.6	0.0	79.1	0.0	40.3	35.0	46.0	Yes				20.0	59.7	No. 8	
No. 30	8.0	4.8	42.7	12.8	92.4	9.2			8.0	0.0	42.7	0.0	50.2	0.0	26.9	15.0	29.0	Yes				13.5	73.2	No. 30	
No. 50	7.0	4.2	35.7	10.7	48.3	4.8			7.0	0.0	35.7	0.0	36.6	0.0	19.7	7.0	20.0	Yes				7.1	80.3	No. 50	
No. 200	1.7	1.0	12.5	3.8	1.4	0.1			1.7	0.0	12.5	0.0	7.4	0.0	4.9	2.0	7.0	Yes				14.8	95.1	No. 200	
# Not within specifications # Not cumulative																									
Lift Thickness, in.:																									
Asphalt Source & Grade:		LION PG 64-22				Binder Percent, (%):		6.0		Asphalt Spec. Grav.:		1.030													
Antistripping Agent:		AKZO KLING BETTA 2550HM				Percent, (%):		1																	

Figure 6-11. SH 24 Overlay Asphalt Mix Design Sheet.

6.2.1 Laboratory Test on Plant Mixes and Field Cores

Both field cores and plant mixes were collected from the selected test section on SH 24. The plant mixes were sampled during construction in July 2009; the field cores were taken in June 2010. The performed laboratory tests on the plant mixes and field cores included:

- Hamburg Wheel Tracking Test (HWTT).
- Overlay Test.
- Repeated Load Test.
- Dynamic Modulus Test.

Figure 6-12 shows the HWTT result. Tables 6-6, 6-7, and 6-8 list the fracture properties, rutting properties, and dynamic modulus values, respectively.

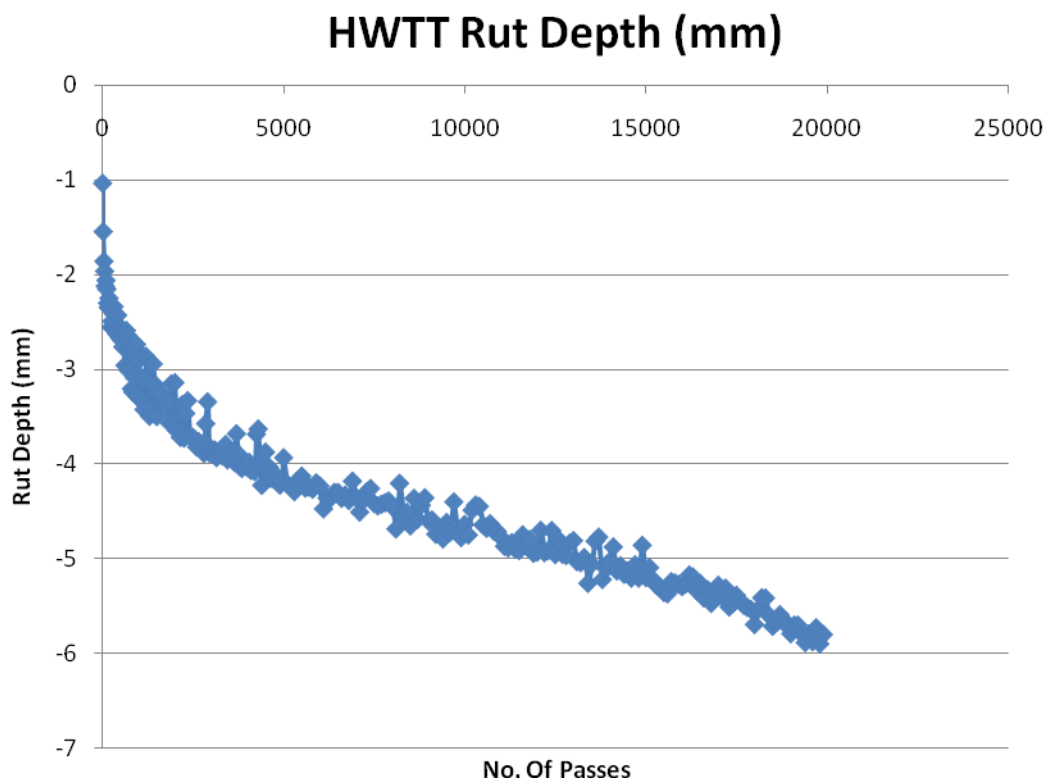


Figure 6-12. HWTT Results.

Table 6-6. Cracking Properties.

	A	n
Field Cores (June 2010)	3.2874E-7	5.0204
Plant Mix Samples	2.7764E-7	4.2794

Table 6-7. Dynamic Modulus Results (ksi)

Temperature (°F)	Frequency (Hz)					
	25	10	5	1	0.5	0.1
14	4208	3897	3654	3189	2976	2403
40	3078	2822	2609	2160	1982	1532
70	1500	1231	1019	668	537	285
100	415	252	175	68	49	22
130	101	55	35	21	15	12

Table 6-8. Rutting Properties.

Temperature(°F)	α	μ
104	0.8588	0.5528

6.2.2 Coefficient of Thermal Expansion Determination for CTB

Since the CTB layer on SH 24 was very thick (11 inches), over-cemented, and fully cracked, it was necessary to investigate the coefficient of thermal expansion of the CTB layer and input it into the TxACOL.

Researchers found no study in Texas or on the national level to measure the CTE of CTB materials, and no standard test procedure is available to measure it. Thus, the researchers developed a simple method within the available tools. First, the researchers used a double-blade saw to cut a CTB core to about 6 inches in length and then glued two metal studs at each end surface. After the samples were put in the temperature chamber for about 24 hours, the researchers used a high-resolution caliper to measure the length between the two ends. Then the chamber temperature was changed for the next temperature, and after another 24 hours, the length was measured again; see Figure 6-13. Three temperatures—2°C, 25°C, and 60°C—were adopted, and the CTE was determined by the linear interpolation method. It was found that the CTB material on SH 24 was 10 microstrain/°C, which is almost the same as that of typical PCC with gravel aggregates. Apparently, more research is needed in this area, since CTE is an

important factor for thermal movement of CTB and, accordingly, thermal reflective cracking in the cold areas of Texas.



Figure 6-13. CTE Measuring of CTB Material.

6.2.3 TxACOL Prediction for SH 24 Test Section

Then, the researchers entered the inputs, such as the pavement structure information and material properties seen in Tables 6-6, 6-7, and 6-8, the CTE information, and the climate information, and accepted the default values for other parameters. Figure 6-14 shows the comparison between the TxACOL-predicted RCR values and field survey results. Figure 6-14 is based on the cracking properties A and n obtained from the OT results of the plant mix samples. Using A and n obtained from field cores on June 2010 would get similar results. Figure 6-15 shows the predicted rut depth by the TxACOL. These rutting prediction results can be regarded as close to the field observation since no rut was observed during the survey.

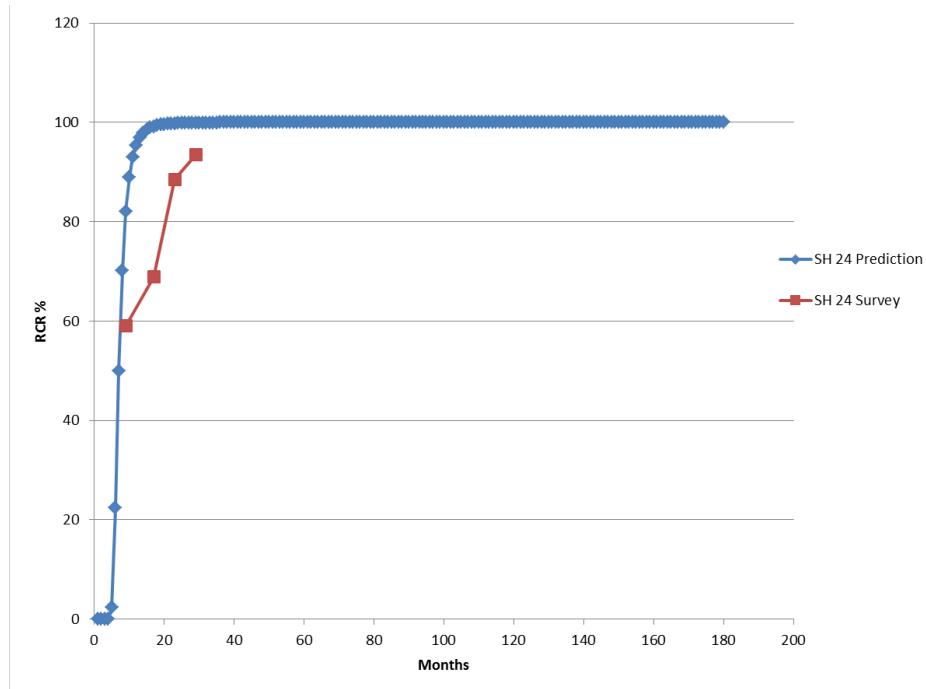


Figure 6-14. RCR Prediction and Survey Result of SH 24 Test Section.

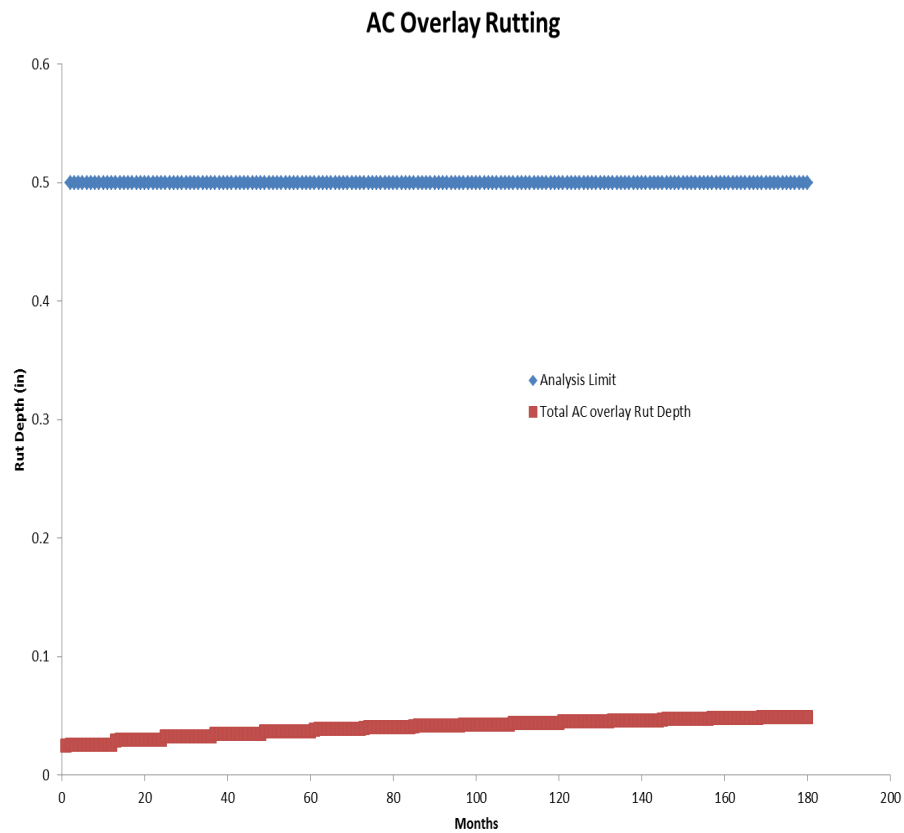


Figure 6-15. SH 24 Rut Prediction Result.

6.3 SUMMARY

Based on the investigation conducted previously, the following summaries are offered:

- The enhanced TxACOL was employed to make predictions for the three test sections on IH 40. For each test section, the fracture properties, A and n , and the dynamic moduli of the overlay mixtures were determined through lab testing of plant mixes; the existing AC layer modulus and the base layer modulus were back-calculated according to the FWD data; and the existing pavement LTE was determined from the FWD data as well.
- The enhanced TxACOL was also employed to make predictions for the test section on SH 24, on which the CTB layer was very thick, over-cemented, and fully cracked. The newly developed thermal SIF model was involved during RCR calculation.
- Based on the comparisons between the enhanced TxACOL predictions and survey results, researchers found that predictions were close to the survey results. It could also be concluded that the new RCR model (ρ - β model) could fit the surveyed RCR curves.
- It was also found that the CTE of the CTB material on SH 24 was 10 microstrain/°C, which is almost the same as that of PCC with gravel aggregates. Such a large CTE can result in large movement of a CTB layer and, consequently, early reflective cracking. Researchers found no study in Texas or on the national level to measure the CTE of CTB materials. Apparently, more research is needed in this area, since CTE is an important factor for thermal movement of CTB and, accordingly, thermal reflective cracking in the cold areas of Texas.

CHAPTER 7.

CONCLUSIONS AND RECOMMENDATIONS

This report documents the pilot implementation of the TxACOL in Texas districts. To facilitate the system implementation in districts, this study developed and conducted district-oriented overlay design workshops; provided asphalt overlay design assistance and monitored the construction of the new overlay projects; performed lab testing for different overlay mixes and updated the material default value database; surveyed the field performance (rutting and cracking) of existing asphalt overlay projects; and enhanced/calibrated the TxACOL. Finally, cases were demonstrated by comparing the enhanced TxACOL prediction with the field survey results.

Based on the research presented in this report, the following conclusions and recommendations are made.

- Both the instructors and trainees benefited from the training workshops, which is very important for the TxACOL enhancement and implementation. District-oriented user training workshops are recommended for any new program implementation.
- Field performance data history surveyed on the 18 test sections showed that:
 - Either thin or thick asphalt overlays can perform well, depending on existing pavement conditions (e.g., LTE), overlay mix, traffic, and climate. Therefore, asphalt overlay including both mix type and thickness should be designed for project-specific service conditions.
 - Asphalt overlay thickness has significant influence on asphalt overlay performance. The overlay thickness has an exponential relationship with asphalt overlay life, so thick overlay is preferred whenever it is possible.
 - Overlay mixes with high RAP can be successfully designed to have similar or better performance than virgin mixes if the balanced mix design procedure is followed.
- Some key input parameters such as dynamic modulus, cracking property, rutting property, FWD modulus, and LTE, have direct impacts on the accuracy of the TxACOL prediction. This report provided guidance on how to obtain reliable and

- representative values of these parameters. Specifically, researchers developed tools and Excel macros to simplify parameter determination processes.
- Default value system is a key part of successfully implementing the TxACOL. Researchers refined and updated default values through assisting different districts on overlay mix design and evaluation.
 - Continuous monitoring and surveying of overlay test sections provides clear cracking and rutting development history. The surveyed RCR results and curves indicate right directions for the TxACOL new models developing and calibration.
 - A new model (ρ - β model) was proposed and incorporated into the TxACOL for predicting RCR. This model fit most of the surveyed RCR curves. The ρ value, which represents the curve width, can be determined directly based on the crack length incremental calculation, while the β value (curve slope) is the calibration factor.
 - A new thermal SIF model was developed and incorporated into the TxACOL to account for the influence of a thick CTB layer's movement under thermal variations.
 - Numerous pilot calculations and sensitivity analysis were conducted under this study, and the calibration factors of the reflective cracking model were refined. The new calibration factors are $\beta = 5.0$, $k_1 = 15$, and $k_2 = 30$. Case analyses showed that the enhanced TxACOL can make reasonable predictions compared to survey results. Apparently, calibration factors need to be further verified through more field test sections.
 - Most of the test sections in this report are recommended to be kept monitored since their cracks are still developing and their RCR values are still increasing.
 - The researchers recommend that the enhanced TxACOL program be used as a design tool for asphalt overlay design in different districts. Asphalt overlays should be designed in parallel with the existing approach and the TxACOL for comparison purposes.

REFERENCES

1. Zhou, F., S. Hu, X. Hu, and T. Scullion, *Mechanistic-Empirical Asphalt Overlay Thickness Design and Analysis System*, FHWA/TX-09/0-5123-3, Texas Transportation Institute, College Station, TX, 2009.
2. AASHTO TP62-03, *Standard Method of Test for Determining Dynamic Modulus of Hot-Mix Asphalt Concrete Mixtures*, 2003.
3. Bonaquist, R., and D. W. Christensen, Practical Procedure for Developing Dynamic Modulus Master Curves for Pavement Structural Design. In *Transportation Research Record: Journal of the Transportation Research Board*, No. 1929, Transportation Research Board of the National Academies, Washington, D.C., 2005, pp. 208–217.
4. Zhou, F., S. Hu, and T. Scullion, *Development and Verification of the Overlay Tester-Based Fatigue Cracking Prediction Approach*, FHWA/TX-07/9-1502-01-8, Texas Transportation Institute, College Station, TX, 2007.
5. Zhou, F., S. Hu, T. Scullion, D. Chen, X. Qi, and G. Claros, Development and Verification of the Overlay Tester Based Fatigue Cracking Prediction Approach, *Journal of Association of Asphalt Paving Technologists*, Vol. 76, pp. 627–662, 2007.
6. Liu, W., and T. Scullion, *MODULUS 6.0 for Windows: User's Manual*, FHWA/TX-05/0-1869-2, Texas Transportation Institute, Texas A&M University, College Station, TX, 2001.
7. Lytton, R. L., F. Tsai, S. Lee, R. Luo, S. Hu, and F. Zhou, *Models for Predicting Reflection Cracking of Hot-Mix Asphalt Overlays*, TRB's National Cooperative Highway Research Program (NCHRP) Report 669, 2010.
8. Hu, S., F. Zhou, and T. Scullion, *Thermal Reflective Crack Propagation*, International Conference on Advanced Characterization of Pavement and Soil Engineering Materials, Athens, Greece, Vol. 2, June 2007, pp. 1173–1182.

